Available online at www.sciencedirect.com

ScienceDirect

Geochimica et Cosmochimica Acta 162 (2015) 202–219

Geochimica et Cosmochimica Acta

www.elsevier.com/locate/gca

The pH of Enceladus' ocean

Christopher R. Glein [a,*,1], John A. Baross [b], J. Hunter Waite Jr. [c]

[a] Geophysical Laboratory, Carnegie Institution of Washington, 5251 Broad Branch Road NW, Washington, DC 20015-1305, United States
[b] Astrobiology Program and School of Oceanography, University of Washington, Seattle, WA, United States
[c] Space Science and Engineering Division, Southwest Research Institute, San Antonio, TX, United States

Received 13 October 2014; accepted in revised form 9 April 2015; available online 16 April 2015

Abstract

Saturn's moon, Enceladus, is a geologically active waterworld. The prevailing paradigm is that there is a subsurface ocean that erupts to the surface, which leads to the formation of a plume of vapor and ice above the south polar region. The chemistry of the ocean is just beginning to be understood, but is of profound geochemical and astrobiological interest. Here, we determine the pH of the ocean using a thermodynamic model of carbonate speciation. Observational data from the *Cassini* spacecraft are used to make a chemical model of ocean water on Enceladus. The model suggests that Enceladus' ocean is a Na–Cl–CO_3 solution with an alkaline pH of ~11–12. The dominance of aqueous NaCl is a feature that Enceladus' ocean shares with terrestrial seawater, but the ubiquity of dissolved Na_2CO_3 suggests that soda lakes are more analogous to the Enceladus ocean. The high pH implies that the hydroxide ion should be relatively abundant, while divalent metals should be present at low concentrations owing to buffering by carbonates and phyllosilicates on the ocean floor. Carboxyl groups in dissolved organic species would be negatively charged, while amino groups would exist predominately in the neutral form. Knowledge of the pH improves our understanding of geochemical processes in Enceladus' ocean. The high pH is interpreted to be a key consequence of serpentinization of chondritic rock, as predicted by prior geochemical reaction path models; although degassing of CO_2 from the ocean may also play a role depending on the efficiency of mixing processes in the ocean. Serpentinization leads to the generation of H_2, a geochemical fuel that can support both abiotic and biological synthesis of organic molecules such as those that have been detected in Enceladus' plume. Serpentinization and H_2 generation should have occurred on Enceladus, like on the parent bodies of aqueously altered meteorites; but it is unknown whether these critical processes are still taking place, or if Enceladus' rocky core has been completely altered by past hydrothermal activity. The presence of native H_2 in the plume would provide strong evidence for contemporary aqueous alteration that replenishes this source of energy for possible life. The high pH also suggests that the delivery of strong oxidants from the surface to the ocean has not been significant (otherwise, sulfuric acid would be produced), which would be consistent with geophysical models of episodic resurfacing activity on Enceladus. This paper represents an expansion of chemical oceanography to an "ocean planet" beyond Earth.

1. INTRODUCTION

A wealth of geological (Smith et al., 1982; Porco et al., 2006, 2014; Spencer et al., 2009), geophysical (Spencer et al., 2006; Schmidt et al., 2008; Howett et al., 2011; Ingersoll and Ewald, 2011; Iess et al., 2014), and geochemical (Postberg et al., 2009, 2011; Waite et al., 2009; Hsu et al., 2015) evidence points to the presence of a global or

* Corresponding author. Tel.: +1 202 478 8967; fax: +1 202 478 8901.
E-mail addresses: cglein@ciw.edu, chris.glein@utoronto.ca (C.R. Glein).
[1] Present address: Department of Earth Sciences, University of Toronto, Earth Sciences Centre, 22 Russell Street, Toronto, ON M5S 3B1, Canada. Tel.: +1 416 978 5508; fax: +1 416 978 3938.

http://dx.doi.org/10.1016/j.gca.2015.04.017
0016-7037/

regional ocean of liquid water beneath the icy crust of the south polar region of Saturn's satellite, Enceladus (Collins and Goodman, 2007; Nimmo et al., 2007; Tobie et al., 2008; Běhounková et al., 2012; Travis and Schubert, 2015). The ocean is believed to be the source of gases, organics, salts, and ices in Enceladus' cryovolcanic plume (Spencer and Nimmo, 2013). Understanding the geochemistry of the ocean is critical for advancing our understanding of the origin and evolution of Enceladus (Zolotov, 2007; Matson et al., 2007; Glein et al., 2008); for gaining insights into geochemical processes on other icy bodies in the outer solar system (Shock and McKinnon, 1993; Kargel et al., 2000; Glein et al., 2009; Sohl et al., 2010; Glein, 2015; Neveu et al., 2015); for comparing aqueous geochemistry on Enceladus to that on the modern and early Earth (Holland, 1984; Sverjensky and Lee, 2010; Pope et al., 2012), Mars (Grotzinger et al., 2014), and asteroids (Zolensky et al., 1999; Brearley, 2006; Zolotov, 2014); for assessing the biological potential of Enceladus (McKay et al., 2008, 2014; Parkinson et al., 2008); and for planning missions to Enceladus (Sotin et al., 2011; Tsou et al., 2012; Lunine et al., 2015) and other worlds where ocean water may be erupting into space (Pappalardo et al., 2013, 2015; Küppers et al., 2014; Roth et al., 2014; Hansen and Kirk, 2015).

The most important compositional variable to understanding the fundamental low-temperature geochemistry of natural waters is the pH (Garrels and Christ, 1965; Drever, 1997), which reflects the acidity of the water and is formally a measure of the thermodynamic activity of the hydrogen ion ($pH = -\log(a_{H+})$) referenced to the infinitely dilute standard state[2] (the second most important variable is the oxidation state; e.g., the reduction potential, Eh). The pH of Enceladus' ocean is currently unknown, although various estimations have been made (Table 1). Zolotov (2007) calculated the pH based on the assumption of chemical equilibrium between water and chondritic rock. However, the robustness of this assumption to icy moons has not been tested. Postberg et al. (2009, 2011) identified $NaHCO_3$ and/or Na_2CO_3 in plume particles, and pointed out that their presence implies a basic pH; but they were unable to pinpoint the pH because of the uncertain carbonate speciation (HCO_3^- vs. CO_3^{-2}). They did suggest a pH of 8.5–9 based on cluster patterns in their mass spectra, but it is unclear if this pH would be consistent with the amount of CO_2 in the plume gas (Waite et al., 2011, 2013). Marion et al. (2012) constructed a speciation model by adding CO_2 to the data of Postberg et al. (2009), but they adopted an unrealistically high partial pressure of CO_2 (see Section 2.2). Recently, it has been suggested that the formation of silica nanoparticles inside Enceladus requires a pH of 8.5–10.5 (Hsu et al., 2015). However, this interpretation is based on a hydrothermal scenario for the formation of the nanoparticles that has received some skepticism, because hydrothermal fluids in equilibrium with chondritic rock may not contain sufficient silica (Zolotov and Postberg, 2014). Direct measurement of the pH of Enceladus' ocean may be possible in the future, but will require a complex and costly drilling mission (Dachwald et al., 2014) to access the liquid.

Table 1
Estimated values for the pH of Enceladus' ocean.

Reference	Value
Marion et al. (2012)	5.7–6.8
Postberg et al. (2009)	8.5–9
Hsu et al. (2015)	8.5–10.5
Zolotov (2007)	10.9
This work	10.8–13.5

Fortunately, a synthesis of chemical data from the *Cassini* spacecraft allows an indirect yet rigorous determination of the pH of Enceladus' ocean. The objective of this paper is to show how spacecraft observations can be used to estimate the pH of an extraterrestrial ocean by linking the latest measurements of carbonate salts in the plume particles (Postberg et al., 2009, 2011) and CO_2 in the plume gas (Waite et al., 2011, 2013) with a thermodynamic model of the carbonate system at the conditions of Enceladus' ocean (Marion et al., 2012). Knowledge of the pH allows a number of important inferences to be made regarding geochemical processes in Enceladus' interior, given that terrestrial experience (Garrels and Christ, 1965; Drever, 1997) demonstrates that the pH of natural waters is controlled by and thus reflects geochemical processes. The pH is also important to the habitability of Enceladus' ocean because the composition of the environment sets boundary conditions for life (McKay et al., 2014).

This paper is structured as follows. In the next section, we derive constraints on the geochemical conditions of Enceladus' ocean from *Cassini* data and interpretations of the data. We then present illustrative (Section 3.1) and realistic (Section 3.2) equilibrium models for the pH and speciation of the ocean. Then, we discuss what the results mean in terms of geochemical processes on Enceladus (Section 4). Lastly, we provide the conclusions of this work.

2. GEOCHEMICAL CONSTRAINTS

2.1. System, temperature, and total pressure

Enceladus presents a unique variation of the well-known problem of carbonate equilibria (Garrels and Christ, 1965). Here, it is assumed that an ocean is the source of the ice grains and gases in Enceladus' plume, as supported by prior studies (Porco et al., 2006, 2014; Schmidt et al., 2008; Postberg et al., 2009, 2011; Waite et al., 2009; Ingersoll and Ewald, 2011; Hsu et al., 2015). Mass spectra obtained by the Cosmic Dust Analyzer (CDA) onboard *Cassini* show that NaCl and $NaHCO_3/Na_2CO_3$ salts are the most abundant non-water constituents in the plume particles (Postberg et al., 2009, 2011). The plume gas is dominated by water vapor (Hansen et al., 2006, 2011), but data from

[2] Conventional thermodynamic standard states (Anderson, 2005) are adopted in the present communication. These correspond to: unit activity of pure water fluid at any temperature and pressure, unit activity of other aqueous species in a hypothetical one molal solution referenced to infinite dilution at any temperature and pressure, and unit fugacity of the hypothetical ideal gas at 1 bar and any temperature.

the Ion and Neutral Mass Spectrometer (INMS) show that it also contains an appreciable amount of CO_2 (Waite et al., 2006, 2009, 2011, 2013), which can explain the presence of solid CO_2 in the south polar region (Brown et al., 2006). Recently, INMS has been flown through the plume several times at lower velocities, which has led to a revision of the composition of the plume gas (Waite et al., 2011, 2013; Bouquet et al., 2015a). Details can be found in the Appendix, but a key result is that the CO_2/H_2O molar ratio has been revised significantly from 6% (Waite et al., 2009) to 0.6% (Waite et al., 2013). The plume compositional data that are relevant to the present paper are given in Table 2.

The simplest geochemical system that is consistent with these observations is Na_2O–HCl–CO_2–H_2O. The components can be written in any manner as long as they correspond to the minimum number of chemical formula units that completely describe the composition of the system (Anderson, 2005). They can but do not need to correspond to real species because they are mathematical constructs that allow application of the phase rule. This is important because the phase rule tells us how much compositional information we need to obtain from the plume to determine equilibrium. Here, the components are written following the convention of Bowers et al. (1984). According to the phase rule, the number of degrees of freedom that are required to determine thermodynamic equilibrium is: $F = C - P + 2$, where C stands for the number of components (=4), and P represents the number of phases (i.e., only the aqueous phase). Therefore, $F = 5$ for this system. The most convenient intensive variables for this problem are temperature, total pressure, the activity of CO_2, and the concentrations of chloride and dissolved inorganic carbon in the ocean. These variables are chosen because it is simple to constrain them using *Cassini* data, and input them into a geochemical speciation model.

Setting the temperature and total pressure is straightforward. The ocean is covered by a layer of water ice (Brown et al., 2006; Iess et al., 2014), so it can be assumed that the two phases are in thermal equilibrium. The temperature should be close to 0 °C unless the ocean is extremely salty or rich in NH_3/CH_3OH, which seems unlikely based on the composition of the plume (Postberg et al., 2009, 2011; Waite et al., 2009, 2011, 2013). The plume gas is envisioned to form when tidally-opened (Hedman et al., 2013; Nimmo et al., 2014) cracks expose ocean water to low pressure (Porco et al., 2006). The newly formed water vapor may be in equilibrium with liquid water; we therefore assume that the total pressure at the interface between the aqueous source and the plume gas is similar to the vapor pressure of water at 0 °C (6.11 mbar; Haynes, 2014). However, chemical equilibrium calculations are performed at a total pressure of 1 bar, because this is the reference pressure at which equilibrium constants are commonly tabulated (Bethke, 2008), and pressure effects are negligible at these low pressures (Marion et al., 2005).

2.2. Activity of carbon dioxide

The activity of CO_2 can be calculated if it is assumed that the CO_2 in the plume gas was in equilibrium with ocean water in the subsurface (Matson et al., 2012). According to Henry's law, $K_H = a_{CO2}/f_{CO2}$; where K_H corresponds to the equilibrium constant ($=10^{-1.1}$ at 0 °C and 1 bar; Shock et al., 1989), a_{CO2} denotes the activity of aqueous CO_2 (often referred to as carbonic acid), and f_{CO2} stands for the fugacity of CO_2. At the low total pressure of interest, the fugacity is essentially identical to the partial pressure (Anderson, 2005). To calculate the activity of CO_2 in the ocean using Henry's law, we first need to constrain the partial pressure of CO_2 at the ocean-vapor interface inside Enceladus. The situation is analogous to carbonate equilibria in surface waters on Earth (e.g., rainwater), where the partial pressure of atmospheric CO_2 controls its aqueous activity (Drever, 1997). In this context, the plume of Enceladus can be thought of as its "atmosphere". However, the situation is actually more complicated because the plume is expanding into the vacuum of space (Hansen et al., 2006), meaning that the partial pressure in the plume is much lower than that at the ocean-vapor interface.

A solution to this problem is to calculate the partial pressure of CO_2 at the ocean-vapor interface using the molar ratio of CO_2/H_2O via Dalton's law: $p_{CO2} = (CO_2/H_2O) \times p_{H2O}$, where p_i refers to the partial pressure of species i. The partial pressure of steam at the ocean-vapor interface can be taken as 6.11 mbar (see Section 2.1). A complication, however, is that the CO_2/H_2O ratio at the ocean-vapor interface should not be the same as that in the plume gas, because steam condenses as its travels through cracks connecting the warm ocean and cold surface of Enceladus (Schmidt et al., 2008; Porco et al., 2014). As a result of this distillation effect, the CO_2/H_2O ratio should be higher in the plume gas than in the source region. This is an important point because it has been assumed that the composition of the plume gas is similar to the source region (Kieffer et al., 2006; Glein et al., 2008; Waite et al., 2009).

Assuming ice–steam equilibrium (Ingersoll and Pankine, 2010), the following mass balance equation can be used to estimate the ratio of CO_2/H_2O gas at the source by accounting for condensation of water vapor during the transport process from the bottom (ocean) to the top (tiger stripes; Spitale and Porco, 2007) of the cracks

$$\rho_{ocean}^{steam} \times (CO_2/H_2O)_{ocean} = \rho_{tiger}^{steam} \times (CO_2/H_2O)_{tiger}, \quad (1)$$

Table 2
Plume composition measurements from *Cassini* INMS or CDA that constrain the carbonate geochemistry of Enceladus' ocean.

Constituent	Measured in	Concentration	Reference
CO_2	Gas phase	0.006 mol/mol H_2O	See Appendix, Bouquet et al. (2015a)
NaCl	Ice grains	0.05–0.2 mol/kg H_2O	Postberg et al. (2009, 2011)
$NaHCO_3 + Na_2CO_3$	Ice grains	0.01–0.1 mol/kg H_2O	Postberg et al. (2009, 2011)

where ρ^{steam} designates the saturation molar density of water vapor at the ocean or tiger stripes, and the CO_2/H_2O ratio at the tiger stripes is taken to be equal to that in the plume gas. Expansion of the gas into a vacuum at the surface should not alter the ratio because no work is performed, and the formation of a significant amount of ice in the plume seems unlikely because there would not be sufficient collisions to nucleate ice in the dilute plume (Schmidt et al., 2008; Hansen et al., 2011), although some ice in the form of nanograins (Jones et al., 2009) may condense at the base of the plume where sufficient collisions occur (Yeoh et al., 2015). This would be important to Eq. (1) if a significant fraction of the ice in the plume exists as nanograins that formed at/above the surface, and if the nanograins are chemically fractionated from the plume gas (i.e., different CO_2/H_2O ratios). This possibility is unconstrained at present, so we will neglect it for the time being; however, dynamical modeling (Yeoh et al., 2015) may allow a quantitative assessment of its importance in the future. Eq. (1) relies upon the assumption that water vapor condenses in the cracks (Schmidt et al., 2008) while CO_2 gas does not, which is probably not completely correct given the reported detection of CO_2 ice in the tiger stripes (Brown et al., 2006). Nevertheless, this equation represents a suitable endmember that reflects the much greater propensity of steam to condense than CO_2, so it should provide a reasonable approximation to the more complex process on Enceladus (see Section 3.2.2.4).

For an ocean temperature of 0 °C (273 K), the ratio of steam densities can be parameterized as: $\log(\rho_{tiger}/\rho_{ocean}) = 9.429–2574/T_{tiger}(K)$, which represents the experimentally determined density ratio (Haynes, 2014) to within ~2% from 153 to 273 K. Combining the previous equations leads to an expression for the activity of CO_2 in the ocean as a function of the CO_2/H_2O ratio in the plume gas, and the temperature of the tiger stripes

$$\log(a_{CO_2}) = \log(CO_2/H_2O)_{plume} + \log(K_H) + \log(p_{H_2O}^{interface}) + \log(\rho_{tiger}/\rho_{ocean}), \quad (2a)$$

$$\log(a_{CO_2}) = \log(CO_2/H_2O)_{plume} + 6.115 - 2574/T_{tiger}(K). \quad (2b)$$

While we presently lack fine-scale information on the temperature distribution of all four tiger stripes, it seems reasonable to assume that average plume material is erupted at a temperature similar to that of Baghdad Sulcus (200 ± 20 K; Goguen et al., 2013), since this tiger stripe appears to be the biggest contributor to the plume (Spitale and Porco, 2007). In light of the uncertainty, however, it would seem prudent to adopt a more conservative temperature range of 170–230 K. Inserting this and $CO_2/H_2O = 0.006$ (Table 2) into Eq. (2b) leads to the constraint that $\log(a_{CO2})$ should be between −11.2 and −7.3. The corresponding partial pressure of CO_2 is $10^{-10.1} – 10^{-6.2}$ bar, which is much lower than the value (0.349 bar) adopted by Marion et al. (2012), who did not account for enrichment of CO_2 in the plume gas by desublimation of water vapor during the process of plume formation (i.e., Eq. (1)), and they assumed that the ocean is in equilibrium with a CO_2 clathrate hydrate. The low activity (~molality) of CO_2 is also inconsistent with the "Perrier Ocean" model of Matson et al. (2012), which requires much more CO_2 to drive bubble formation. On the other hand, an analysis of data presented graphically by Zolotov (2007) indicates a consistent CO_2 activity of $10^{-7.4}$ at 0 °C.

2.3. Concentrations of chloride and carbonate

Geochemical and geophysical approaches can be used to constrain the chloride concentration in Enceladus' ocean. Postberg et al. (2009, 2011) identified peaks in CDA mass spectra of salt-rich plume particles that they attributed to NaCl-bearing clusters. They also attempted to reproduce the CDA data by performing laboratory experiments with a laser, and found that solutions with 0.05–0.2 mol of NaCl per kg of water can produce spectra that are consistent with those from Enceladus (Postberg et al., 2009). This represents a possible range for the chloride concentration in the ocean if the salt-rich plume particles are formed from flash freezing of aerosolized ocean water (Spencer and Nimmo, 2013). However, there are caveats that may preclude direct application of the laboratory data to Enceladus. First, water vapor may condense onto ice grains as they are transported to the surface (Schmidt et al., 2008). The apparent concentration of chloride may be lower than the actual concentration in the ocean, so the reported range should be treated as a lower limit (Postberg et al., 2009). Second, the laser experiments may not provide a completely accurate representation of the impact ionization process at Enceladus. Postberg et al. (2009) argue otherwise, but it is impossible to know for sure unless calibration curves for impact and laser ionization of salt-bearing solutions/ices can be compared. Based on this discussion, the range 0.05–0.2 molal Cl^- should be regarded as a useful but not rigid constraint on the geochemistry of Enceladus' ocean.

An alternative approach is to estimate the chloride concentration from the size of the ocean (Glein and Shock, 2010). Chloride is known as a conservative species because it is very stable in liquid water, and is generally not incorporated into minerals except under arid conditions (Drever, 1997). This is useful behavior because the concentration of chloride in solution simply depends on the total amount of chloride and the mass of water. The next step is to estimate how much chloride there is on Enceladus, and the mass of its ocean.

The total amount of chloride can be estimated from the mass of rock, as Enceladus most likely accreted chloride in rocky material (Sharp and Draper, 2013; Bockelée-Morvan et al., 2014). Iess et al. (2014) recently determined the gravity field of Enceladus, and found the mean moment of inertia to be consistent with a differentiated interior having a rocky core of density 2400 kg m^{-3} and radius 192 km. This implies a mass of rock of 7.1×10^{19} kg. The modeled core density is in close agreement with the grain density of the CI chondrite Orgueil (2420 ± 60 kg m^{-3}; Macke et al., 2011), which suggests that CI chondrites may be a reasonable analogue for the bulk chemistry of Enceladus' core. If Enceladus accreted rocks with a chloride content similar to CI chondrites (700 ppm; Lodders, 2003), then the total amount of chloride on Enceladus would be

1.4×10^{18} mol. All or at least most of this can be expected to be dissolved in the ocean because the relatively low core density implies the presence of abundant hydrated silicates that are indicative of extensive water–rock interaction (see Section 4.3), and chloride would be leached into the water during aqueous alteration of the core (Zolotov, 2007, 2012). A total extraction scenario represents a plausible endmember, but it is possible that some of the chloride is not in the ocean; and could have been lost to Saturn's E ring, or trapped in the ice shell of Enceladus after being delivered there inside plume particles (Postberg et al., 2009, 2011).

Next, we need to estimate the mass of ocean water. Glein and Shock (2010) presented a structural model where the ocean is treated as a cap of uniform thickness that resides on top of the rocky core, and is centered on the geologically active south pole (Porco et al., 2006). The ocean can be a global or regional body of water (Collins and Goodman, 2007; Tobie et al., 2008; Běhounková et al., 2012) depending on how far north it extends in latitude (LAT; northern latitudes are positive, whereas southern latitudes are negative). While this model is a simplification (a more realistic ocean may be thickest beneath the south pole, becoming thinner at more northern latitudes; Iess et al., 2014), it allows a first-order estimate of the ocean's volume to be computed using a simple analytical expression (Glein and Shock, 2010)

$$V_{\text{ocean}} = (2\pi/3)[r_{\text{ocean}}^3 - r_{\text{core}}^3][1 - \cos(\text{LAT} + 90^\circ)], \quad (3)$$

where the radius of the core is taken to be 192 km (Iess et al., 2014), and the radius of the ocean is related to Enceladus' mean radius ($R = 252$ km) and the thickness of ice above the ocean by $r_{\text{ocean}} = R - h_{\text{ice}}$. The mass of ocean water can be obtained by multiplying its volume and density, the latter assumed to be similar to that of pure liquid water (1000 kg m^{-3}).

The molal concentration of Cl^- in Enceladus' ocean can now be calculated as a function of the latitudinal extent of the ocean and the thickness of overlying ice

$$m_{Cl^-} = (6.7 \times 10^5)\left[(R - h_{\text{ice}})^3 - r_{\text{core}}^3\right]^{-1} \times [1 - \cos(\text{LAT} + 90^\circ)]^{-1}, \quad (4)$$

where the radii and ice thickness are expressed in units of kilometers. Fig. 1 shows that the Cl^- concentration is inversely related to the size of the ocean (Glein and Shock, 2010). As long as the ice shell remains salt-free (Zolotov, 2007), the Cl^- concentration will increase as the ice above the ocean thickens, and as the ocean becomes localized to more southern latitudes.

Limits on the structure of the ocean can be derived from geophysical and geological arguments. Iess et al. (2014) suggested that isostatic compensation is taking place at the base of a layer of ice floating on Enceladus' ocean, and they estimated that the ice layer should be 30–40 km thick. The latitudinal extent of the ocean is presently unknown (Iess et al., 2014), but a reasonable estimate is to assume that it underlies at least the active south polar region (Porco et al., 2006; Iess et al., 2014), and it may extend as far north as the equator (Tobie et al., 2008; Běhounková et al., 2012; Spencer and Nimmo, 2013). This leads to a constraint of $-50^\circ < \text{LAT} < 0^\circ$. An ocean that underlies a significant portion of the northern hemisphere or a global ocean seems unlikely (but not impossible) because the heavily cratered northern hemisphere has been less geologically active than the southern hemisphere (Spencer et al., 2009), and their morphological differences can be attributed to the absence of a subsurface ocean and associated tidal heating in the northern hemisphere (Tobie et al., 2008). Another argument against an ocean at LAT > 0° is the difficulty in preventing a large ocean from freezing over geologic timescales (Roberts and Nimmo, 2008). Altogether, the geophysical approach suggests that Enceladus' ocean can be assumed to contain 0.2–1.2 molal Cl^- (Fig. 1). Like for the geochemical approach, this should be regarded as a useful but not rigid constraint.

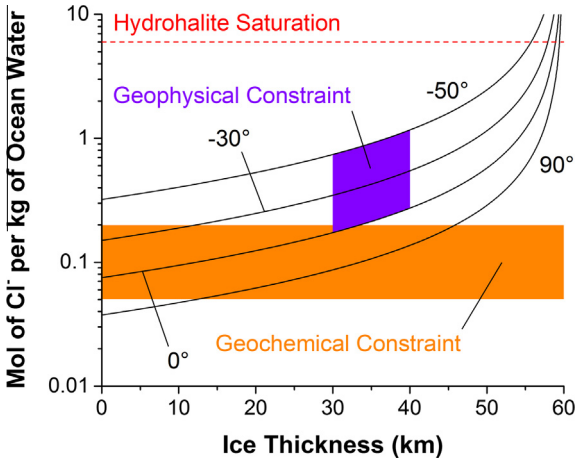

Fig. 1. The concentration of chloride in Enceladus' ocean as a function of the thickness of water ice above the ocean. The curves show results for models with an ocean underlying all latitudes south of the indicated value (e.g., a global ocean corresponds to 90°). The region labeled "Geophysical Constraint" is consistent with Airy compensation depths or ice thicknesses inferred by Iess et al. (2014), and with a south polar (LAT = −50°; Iess et al., 2014) or southern hemispheric (LAT = 0°) ocean as suggested by the more active geology of the southern hemisphere compared to the northern hemisphere (Spencer et al., 2009; Spencer and Nimmo, 2013). The region labeled "Geochemical Constraint" indicates the concentration range deduced by Postberg et al. (2009, 2011) for the plume particles. The dashed horizontal line shows the approximate concentration where hydrohalite ($NaCl{\cdot}2H_2O$) would precipitate from the ocean (Marion et al., 2010).

The geochemical approach indicates that the ocean should contain 0.05–0.2 molal Cl^-, while the geophysical approach predicts 0.2–1.2 molal Cl^- (Fig. 1). Therefore, the most likely value may be 0.2 molal. In recognition of the uncertainties, however, the entire range (0.05–1.2 molal Cl^-) will be considered. This range is much lower than the saturation concentration (~6 molal) of hydrohalite ($NaCl{\cdot}2H_2O$; Fig. 1), which supports the expectation of conservative behavior for chloride inside Enceladus (Glein and Shock, 2010).

The concentration of dissolved inorganic carbon ($DIC = CO_2(aq) + \sum HCO_3^- + \sum CO_3^{-2}$) in the ocean can

be estimated from the DIC/Cl molar ratio in the plume particles. Postberg et al. (2009) found that mass spectra of salt-rich plume particles can be reproduced from laboratory solutions containing 2–5 times more Cl^- than DIC. As discussed above, there is the question of whether these experiments provide a realistic simulation of the eruption and detection processes at Enceladus. On the other hand, the ratio should be more robust than the absolute concentration because of canceling effects. As an example, condensation of steam on plume particles (Schmidt et al., 2008) would decrease the DIC concentration of the particles, but the concentration of Cl^- would decrease correspondingly, such that the DIC/Cl ratio would not change. Likewise, the detector response at Enceladus could differ from that in the laboratory, but the change in response for chloride and carbonate species may be similar, such that the ratio at Enceladus can be derived using laboratory data. However, this cancellation may not be perfect, so a conservative DIC/Cl ratio of 0.1–1 can be adopted to (plausibly) encompass the actual value. This would lead to a possible range of 0.005–1.2 molal for the DIC concentration, with a preferred range of 0.04–0.1 molal for the nominal case of 0.2 molal Cl^-.

3. CARBONATE SPECIATION MODELS

3.1. System Na_2O–CO_2–H_2O

3.1.1. Method

The simplest starting point for elucidating the geochemistry of Enceladus' ocean is to compute chemical equilibrium between aqueous CO_2, HCO_3^-, and CO_3^{-2} at the ocean-vapor interface (for the purpose of computing the pH, we can neglect the Na^+ that must be present to satisfy charge balance). This textbook case of carbonate speciation (Garrels and Christ, 1965; Drever, 1997) can be represented by the following chemical equations

$$CO_2(aq) + H_2O(l) \leftrightarrow HCO_3^-(aq) + H^+(aq), \quad (5)$$

$$HCO_3^-(aq) \leftrightarrow CO_3^{-2}(aq) + H^+(aq), \quad (6)$$

and the law of mass action leads to the corresponding equilibrium constant expressions

$$K_5 \approx m_{HCO_3^-} a_{H^+} / a_{CO_2} = 10^{-6.56} \text{ (at 0 °C, 1 bar)}, \quad (7)$$

$$K_6 \approx m_{CO_3^{-2}} a_{H^+} / m_{HCO_3^-} = 10^{-10.62} \text{ (at 0 °C, 1 bar)}, \quad (8)$$

where m_i stands for the molal concentration of species i. These equations are approximately correct because the water is assumed to be pure ($a_{H2O} = 1$), and ideal behavior is also assumed (activity = molality); these are the conventional assumptions (Stumm and Morgan, 1996).

We can calculate the pH using Eqs. (7) and (8), the activity of CO_2, and the molality of dissolved inorganic carbon in Enceladus' ocean

$$m_{DIC} \approx m_{HCO_3^-} + m_{CO_3^{-2}}. \quad (9)$$

Eqs. (7)–(9) can be combined and the resulting quadratic solved to express the activity of H^+ as a function of the activity of CO_2 and the molality of DIC

$$a_{H^+} \approx 0.5\left(K_5 a_{CO_2} + \sqrt{K_5^2 a_{CO_2}^2 + 4K_5 K_6 m_{DIC} a_{CO_2}}\right) m_{DIC}^{-1}. \quad (10)$$

Lastly, the pH of the ocean can be calculated from the definition, $pH = -\log(a_{H+})$.

3.1.2. Results and discussion

Fig. 2 shows the ocean pH for this geochemical model. The pH is predicted to increase with the DIC concentration, and decrease with increasing activity of CO_2. The pH is a linear function of $\log(a_{CO2})$ at the most negative values of this quantity. At these conditions, HCO_3^- is not important to the speciation, where essentially all of the inorganic carbon exists as CO_3^{-2} because of the high pH. In this regime, the pH can be written as

$$pH \approx 0.5\log(m_{DIC}) - 0.5\log(K_5) - 0.5\log(K_6) - 0.5\log(a_{CO_2}). \quad (11)$$

The pH of Enceladus' ocean can be approximated by adopting the constraints on the activity of CO_2 and molality of DIC (see Sections 2.2 and 2.3). Based on what is considered the most probable range in the DIC concentration (0.04–0.1 molal), this model gives a pH of 12.6 ± 1.1 (Fig. 2). If it is assumed that the DIC concentration is known to less certainty (0.005–1.2 molal), then the uncertainty in the computed pH would increase somewhat ($pH = 12.6 \pm 1.6$; Fig. 2). It must be emphasized that these are illustrative values because the present model provides a simplified description of the carbonate system (see Section 3.2.2.1).

Nevertheless, this model allows several key generalizations to be made. First, the ocean should be strongly basic (Fig. 2). For the ocean to instead have a circumneutral pH, Enceladus' plume gas would need to be composed almost entirely of CO_2 (Eq. (2b)), which is not the case (Waite et al., 2006, 2009, 2011, 2013). The geochemical factor that is most indicative of the high pH is the low activity of CO_2. This quantity is also responsible for most of the uncertainty in the derived pH (Fig. 2), which can be traced back to uncertainty in the temperature of the tiger stripes (Eq. (2b); Goguen et al., 2013). The high pH implies that the carbonate-bearing cluster ($Na_3CO_3^+$) identified by Postberg et al. (2009, 2011) in the plume particles was derived from aqueous carbonate, as opposed to the bicarbonate ion. In terms of its geochemistry, Enceladus' ocean is a Na–Cl–CO_3-type water (Deocampo and Jones, 2014), similar to but also different from Na–Cl–Mg–SO_4 seawater on Earth (Garrels and Thompson, 1962).

It may seem remarkable that a high pH solution can generate a plume containing CO_2 (Waite et al., 2011, 2013), a weakly acidic gas; but irreversible removal of CO_2 from the system by degassing and loss to space drives the following reaction forward

$$CO_3^{-2}(aq) + 2H^+(aq) \rightarrow CO_2(g) + H_2O(l). \quad (12)$$

The ocean–plume system is thus demonstrating Le Chatelier's principle on a large scale. This equation also shows that CO_2 degassing can raise the pH, which commonly occurs when carbonate-saturated groundwaters in equilibrium with elevated fugacities of CO_2 emerge as

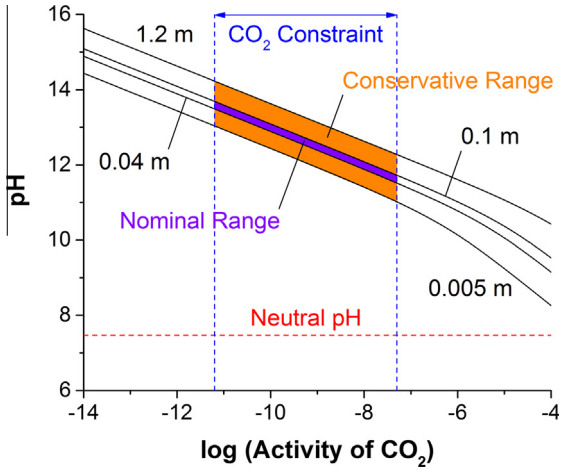

Fig. 2. The pH of Enceladus' ocean from a simplified model of carbonate speciation at 0 °C and 1 bar. The curves show the derived pH at the indicated (molal) concentration of dissolved inorganic carbon. The constraint on the activity of CO_2 is from Section 2.2. The orange region shows where the ocean would be for the conservative range in DIC from Section 2.3, while the violet region is consistent with the preferred range. The violet region is overlaying a portion of the orange region. For comparison, the pH of neutral water at this temperature and total pressure is 7.47 (Shock et al., 1997). (For interpretation of the references to colour in this figure legend, the reader is referred to the web version of this article.)

springs at the Earth's surface (Choi et al., 1998; Hammer et al., 2005). Thus, CO_2 degassing may contribute to the high pH of ocean water on Enceladus, but the key controller of the pH is likely to be water–ultramafic rock interactions and mineral buffering (see Sections 4.1 and 4.3).

3.2. System Na_2O–HCl–CO_2–H_2O

3.2.1. Method

The pH of Enceladus' ocean can be determined as accurately as presently possible by making a chemical model that accounts for equilibrium among all aqueous species (Garrels and Thompson, 1962). This is done here by performing calculations of chemical equilibrium at 0 °C and 1 bar using the SpecE8 program, which is part of the Geochemist's Workbench® 6 software package (Bethke, 2008). This program calculates the activities and concentrations of aqueous species that satisfy all of the mass action equations in the system, as well as conservation of mass and charge balance. The present system contains the following 13 species: Cl^-, CO_2(aq), CO_3^{-2}, H^+, HCl, HCO_3^-, H_2O, Na^+, NaCl, $NaCO_3^-$, $NaHCO_3$, NaOH, and OH^-. Equilibrium constants are taken from the thermo.dat database that is included with the Geochemist's Workbench®. This database is based on the SUPCRT database (Johnson et al., 1992). The system is treated as a non-ideal solution, and activity coefficients are computed using the B-dot equation of Helgeson (1969), which is an empirically extended form of the Debye–Hückel equation. The B-dot equation is thought to be reasonably accurate for ionic strengths up to ~1 molal (Bethke, 2008). The activity coefficients of neutral solutes are set to unity (Anderson, 2005). Oxidation–reduction reactions (Glein et al., 2008) and reactions involving minerals (Zolotov, 2007) do not need to be considered to calculate the pH of the ocean, because the analytical data from Enceladus are sufficient in this chemical system (see Section 2.1). SpecE8 uses the Newton–Raphson method to find the equilibrium distribution subject to the constraints on the activity of CO_2 (see Section 2.2) and the concentrations of chloride and dissolved inorganic carbon (see Section 2.3), with Na^+ serving as the counterion (Postberg et al., 2009).

3.2.2. Results and discussion

3.2.2.1. The pH. Fig. 3 shows the ocean pH at (A) low, (B) nominal, and (C) high Cl^- concentrations for this geochemical model. The pH curves in Fig. 3 are very similar to those in Fig. 2, which makes sense because the simplified model in Section 3.1.1 captures the essentials of the carbonate geochemistry that are elaborated in the more sophisticated and realistic model. The models differ, however, in their quantitative details; the present model gives pH values that are slightly lower than those from the previous model ($\Delta pH \approx 0.2$–0.7). The pH difference depends on composition; and becomes larger with increasing concentrations of Cl^- and DIC, because the second-order effects of solution non-ideality and complex formation (e.g., $Na^+(aq) + CO_3^{-2}(aq) \leftrightarrow NaCO_3^-(aq)$) become more important. Nevertheless, the analytical model (Eq. (10)) provides a reasonable approximation, and can be a useful tool for planetary geochemistry.

The nominal case indicates that Enceladus' ocean should have a pH of 12.2 ± 1.1 (Fig. 3B). However, a comprehensive analysis of the compositional space suggests that the pH could be as low as 10.8 (Fig. 3A) or as high as 13.5 (Fig. 3C). This leads to a more conservative estimate of the $pH = 12.2 \pm 1.4$ (Table 1). The more accurate speciation model reinforces the conclusion that Enceladus' ocean should be strongly basic. Thus, the ocean is clearly different from terrestrial seawater ($pH \approx 8.1$; Garrels and Thompson, 1962), which is in chemical communication with a much larger reservoir of CO_2 gas ($p_{CO2} \approx 4 \times 10^{-4}$ bar).

The present pH is similar to those (~11; ~12) predicted by Zolotov (2007) for Enceladus' ocean and Zolensky et al. (1989) for fluids in the parent bodies of CM chondrites, respectively, from reaction path models of aqueous alteration of chondritic rock at 0 °C. It is considerably higher than the value (~6–7) estimated by Marion et al. (2012) from a thermodynamic analysis similar to the present one. Yet, the Marion et al. (2012) model was based on an assumed partial pressure of CO_2 in the ocean that is unrealistically high (see Section 2.2), which led to the weakly acidic pH. The present pH is also higher than that (8.5–9) suggested by Postberg et al. (2009) from their interpretation of *Cassini* CDA data for reasons that have yet to be identified. Our value is consistent with both the CDA and INMS data, although the high pH is determined primarily by the abundance of CO_2 in the plume gas from INMS, and by our model of how its partial pressure changes from the plume/tiger stripes to the liquid water source region (i.e.,

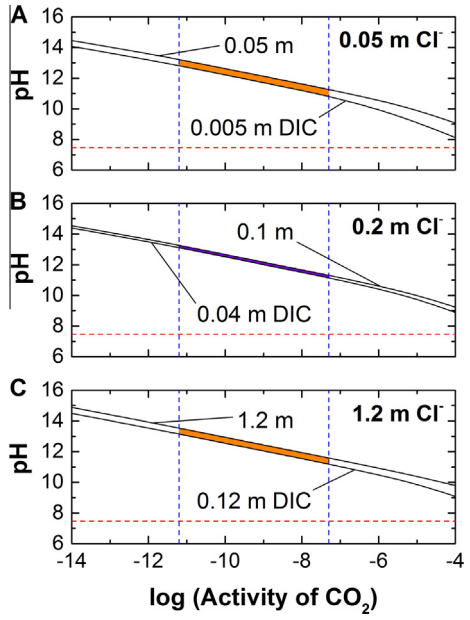

Fig. 3. The pH of Enceladus' ocean from a detailed model of carbonate speciation at 0 °C and 1 bar, and a chloride concentration of (A) 0.05 molal; (B) 0.2 molal; and (C) 1.2 molal. The curves show the derived pH at the indicated concentration of dissolved inorganic carbon. The area between the dashed vertical lines represents the constraint on the activity of CO_2 from Section 2.2. The orange region shows where the ocean would be for the conservative range in DIC (DIC/Cl = 0.1–1) from Section 2.3, while the violet region is consistent with the nominal model (DIC/Cl = 0.2–0.5). The dashed horizontal line indicates the pH = 7.47 of neutral water at this temperature and total pressure (Shock et al., 1997). (For interpretation of the references to colour in this figure legend, the reader is referred to the web version of this article.)

Eq. (1)). The present pH may be more robust given that it is more consistent with what is expected for water–chondrite equilibrium at 0 °C (Zolensky et al., 1989; Zolotov, 2007, 2012). This can also be taken as an argument against the low end of the pH range (8.5–10.5) put forth by Hsu et al. (2015) from their model of nanosilica synthesis. However, the high end of their range may be consistent with our value considering the uncertainties involved (see Section 3.2.2.4).

3.2.2.2. Speciation. Fig. 4 shows the chemical speciation that corresponds to the results in Fig. 3. Na^+ is computed to be the most abundant inorganic species in Enceladus' ocean, consistent with its ubiquity in the plume particles (Postberg et al., 2009, 2011); and Cl^- should be the most abundant anion in the ocean. The model implies that the ocean is dominated by an NaCl component, like terrestrial seawater (Garrels and Thompson, 1962). This attests to the great thermodynamic stability of these species in liquid water (Shock et al., 1997). Indeed, the free energy minimization calculations of Zolotov (2007, 2012) predict that NaCl should be the most abundant solute component in aqueous fluids on small chondritic bodies, such as Enceladus.

Unlike seawater (<1 mmolal; Garrels and Thompson, 1962), however, the Enceladus ocean is expected to contain a significant amount of the carbonate ion, where the carbonate speciation in the constrained range of a_{CO2} depends on the concentrations of Cl^- and DIC (Fig. 4). At lower concentrations of Cl^- and DIC, CO_3^{-2} is predicted to be the dominant form of DIC (Fig. 4A–D); while $NaCO_3^-$ would be more abundant at higher Cl^- and DIC concentrations (Fig. 4E–F), because formation of the complex is driven by higher concentrations of Na^+ at these conditions. The source of the relatively high carbonate concentration may be dissolution of a relatively soluble carbonate mineral, such as gaylussite ($Na_2Ca(CO_3)_2{\cdot}5H_2O(s) \leftrightarrow CaCO_3(s) + 5H_2O(l) + 2Na^+(aq) + CO_3^{-2}(aq)$), which is found in soda lakes on Earth (Bischoff et al., 1991). Carbonate minerals may have formed on Enceladus when CO_2-bearing ices (Ootsubo et al., 2012) melted and reacted with silicate minerals (Zolotov, 2012). Mineralogical and isotopic evidence demonstrate that such chemistry also occurred on the parent bodies of numerous chondrites (Brearley and Jones, 1998; Grady et al., 2002; Alexander et al., 2015).

The carbonate-rich composition draws attention to terrestrial soda lakes (Garrels and Mackenzie, 1967; Jones et al., 1977; Eugster and Hardie, 1978; Bischoff et al., 1993; Kempe and Kazmierczak, 2002) as possessing a similar geochemical feature to the Enceladus ocean. It would not be improper to call Enceladus' ocean a "soda ocean", and we suggest that geochemical and microbiological studies of soda lakes on Earth (e.g., Mono Lake in the Great Basin or Lake Magadi in the East African Rift Valley) may provide useful insights into the geochemistry and possible biology of Enceladus' ocean. For example, although we presume that freezing controls the salinity of the ocean (see Section 2.3), evaporation (via the plume) could play an important role in the geochemical evolution of the ocean, like in terrestrial soda lakes (Garrels and Mackenzie, 1967). Soda lakes are among the most biologically productive bodies of water on Earth because of high rates of photosynthesis, and most are stratified with respect to O_2 (Sorokin et al., 2014). On Enceladus, photosynthesis would not be possible, but geochemical sources of energy could sustain an anaerobic ecosystem (McKay et al., 2008) in an ocean that contains an abundant source of inorganic carbon. These examples show that the soda lake analogy deserves further study, but we will now move on because terrestrial soda lakes (pH ≈ 9–10.5) are generally not quite as basic as the Enceladus ocean (pH = 12.2 ± 1.4), and our goal is to find a closer match (see Section 4.1). It is not (known) Antarctic lakes because, while physically analogous to Enceladus' ocean, they are apparently less geochemically relevant because of their much lower pH (~6–8; Murray et al., 2012; Christner et al., 2014).

The relatively high carbonate concentration should limit (via the common ion effect) the oceanic concentrations of many metals (particularly Ca, Mn, Sr, Ba) that can be incorporated into carbonate minerals, as exemplified by the following equilibrium

$$CaCO_3(calcite) \leftrightarrow Ca^{+2}(aq) + CO_3^{-2}(aq). \quad (13)$$

This example implies that the activity of Ca^{+2} in Enceladus' ocean would be $\sim 4 \times 10^{-7}$ (Johnson et al., 1992) for a representative CO_3^{-2} activity of 0.01, and the corresponding concentration of Ca^{+2} would be of order μmolal, which is several orders of magnitude lower than in seawater (~6000 μm; Garrels and Thompson, 1962).

The high pH of ~12 should lead to trace levels of other metals (e.g., Mg, Fe, Ni, Zn) in the Enceladus ocean. This is because these metals can be sequestered in phyllosilicate or hydroxide minerals in the rocky core (Zolotov, 2007, 2012; Iess et al., 2014; Neubeck et al., 2014; Hsu et al., 2015), and their release into ocean water requires acid hydrolysis, as illustrated in the example below

$$2Mg_3Si_2O_5(OH)_4(\text{chrysotile}) + 6H^+(aq) \leftrightarrow Mg_3Si_4O_{10}(OH)_2(\text{talc}) + 6H_2O(l) + 3Mg^{+2}(aq), \quad (14)$$

which suggests that the equilibrium concentration of Mg^{+2} in the ocean should be very low (~10–100 nmolal; Johnson et al., 1992), many orders of magnitude lower than in seawater (~40 mm; Garrels and Thompson, 1962).

Because the pH of Enceladus' ocean is so high (Fig. 3), bicarbonate species should be only minor constituents of the ocean (Fig. 4). In contrast, the hydroxide ion is expected to be one of the more abundant species in the ocean. This means that base-catalyzed reactions may be important to the synthesis (Proskurowski et al., 2008; Lang et al., 2010), transformation (Cody et al., 2011), and degradation (e.g., hydrolysis of nitriles, esters, etc.) of potential organic compounds (Postberg et al., 2008; Waite et al., 2009, 2011, 2013) in the ocean. Base catalysis may allow various species to reach equilibrium with respect to water addition. Therefore, anomalously high concentrations of water soluble but hydrolytically labile compounds (e.g., urea, acetyl thioesters) in the plume would imply active production to counteract hydrolysis, suggesting dynamic organic or biochemistry inside Enceladus.

To help guide future data analysis, experimentation, modeling, and mission planning, Table 3 provides a summary of what are suggested to be the most consistent speciation models of Enceladus' ocean, based on current chemical information.

3.2.2.3. Organics. The pH of the ocean has major consequences for the stability of organic compounds with acidic

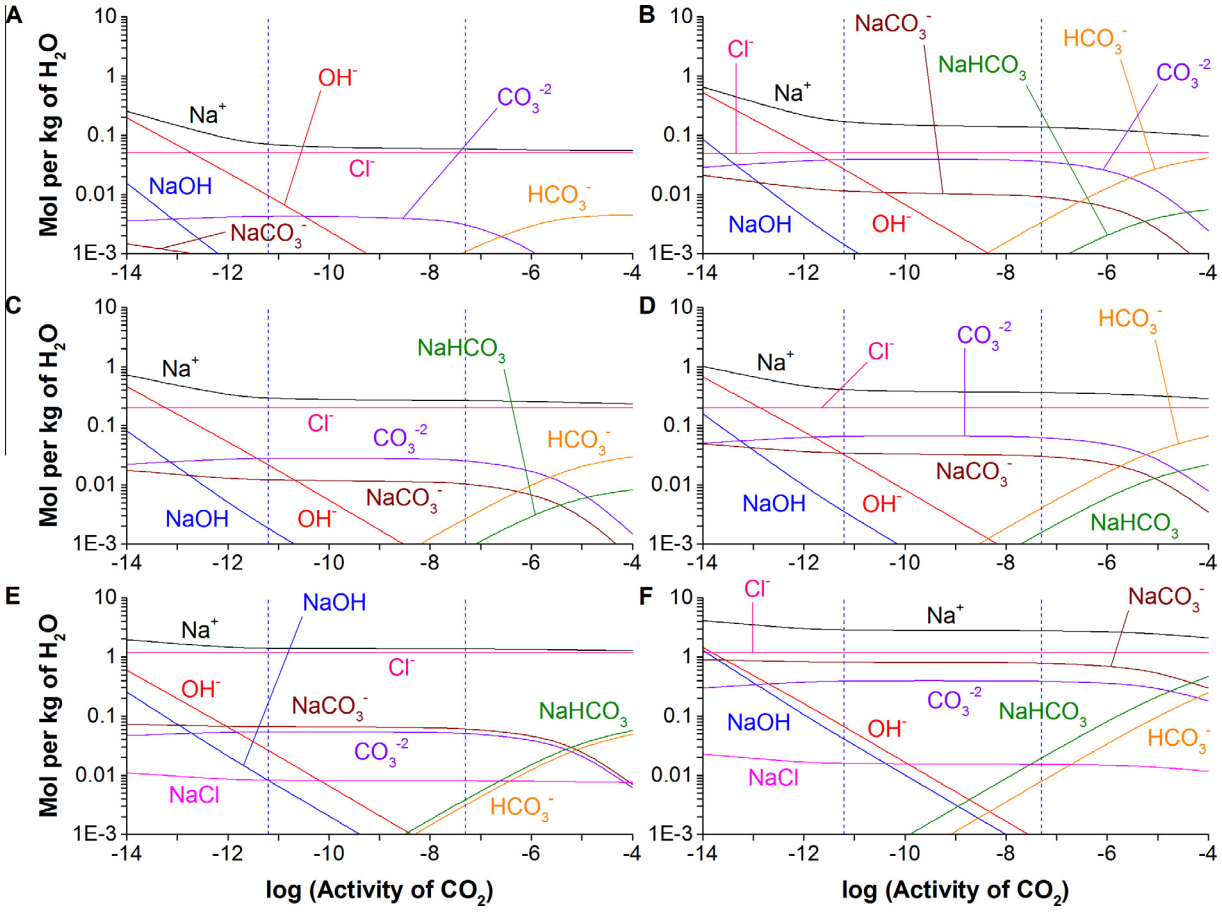

Fig. 4. Derived concentrations of major chemical species in Enceladus' ocean from a detailed model of carbonate speciation at 0 °C and 1 bar, for constraints (see Section 2.3) of (A) 0.05 molal Cl^- and DIC/Cl = 0.1; (B) 0.05 molal Cl^- and DIC/Cl = 1; (C) 0.2 molal Cl^- and DIC/Cl = 0.2; (D) 0.2 molal Cl^- and DIC/Cl = 0.5; (E) 1.2 molal Cl^- and DIC/Cl = 0.1; and (F) 1.2 molal Cl^- and DIC/Cl = 1. Plots (A), (B), (E) and (F) encompass the conservative range in the concentrations of Cl^- and DIC, while plots (C) and (D) span the preferred concentration range. The region between the dashed vertical lines represents the constraint on the activity of CO_2 from Section 2.2.

or basic functional groups (Schulte and Shock, 2004). At 0 °C and pH = 12, carboxylic acids ($pK_a \approx 5$; Shock, 1995) would exist almost exclusively as the deprotonated carboxylate anions (e.g., acetate), but an appreciable fraction (~10%) may be present as Na-complexes (Shock and Koretsky, 1993). Amines ($pK_a \approx 11$; Shock et al., 1997), meanwhile, would exhibit the opposite behavior. Most amine molecules would exist in the neutral form (e.g., CH_3NH_2), although a non-negligible fraction (~10%) would be present as the protonated aminium cations (e.g., $CH_3NH_3^+$).

These effects are important to searches for ocean-derived organic compounds in Enceladus' plume (Waite et al., 2009). Ionized organics behave like inorganic salts, so they would be non-volatile at 0 °C, and should not degas from the ocean. This is in contrast to neutral species that can go into the plume gas. Organic acids from the ocean would be frozen inside the plume particles (Postberg et al., 2008, 2009, 2011), while ocean-derived amines may be detectable in the plume gas (e.g., NH_3; Waite et al., 2009, 2011, 2013). The present examples may be of special interest, as acetate is the most abundant water-soluble organic species in carbonaceous chondrites (Yuen et al., 1984), and methylamine has been detected in comet Wild 2 samples (Glavin et al., 2008).

Simple amino acids (like those in meteorites and comets; Pizzarello et al., 2006; Elsila et al., 2009) with one carboxyl and one amino group (e.g., glycine) should exist predominately as aqueous monoanions, so they would be present in the plume particles and not in the gas phase if they are derived from Enceladus' ocean. *In situ* (Lunine et al., 2015) and sample return (Tsou et al., 2012) methods will need to be developed to access and analyze astrobiologically interesting organic salts that would be embedded in ice grains (Kirby et al., 2014).

3.2.2.4. Other factors. The simple model of the pH is informative, but it may have additional uncertainties that are not captured by the error bars. One process that could change the computed pH is if some of the CO_2 that is degassed from ocean water condenses in the tiger stripes during the eruption process, as is evidently the case (Brown et al., 2006). The plume gas would contain less CO_2 than it should in terms of the model, so the activity of CO_2 in the ocean would be higher than adopted, which would lead to a pH lower than calculated (Fig. 3). It is difficult to determine how large this effect might be, but we are inclined to regard it as minor because the pH is not sensitive to a_{CO2}. In fact, an increase in a_{CO2} by an order-of-magnitude would decrease the pH by approximately half a unit (Eq. (11)). So, ~99% of the ocean-derived CO_2 would need to be removed from the plume gas for the calculated pH to decrease by one unit. CO_2 condensation would thus appear to be a second-order effect, unless >99.99% of the CO_2 snows out, which may be unlikely because CO_2 is quite volatile (e.g., its triple point pressure is 5.18 bar at 216.6 K; Lemmon et al., 2010).

We can also consider the effect of CO_2 condensation in the limit of no distillation (see Section 2.2), where CO_2 would need to freeze out at the same rate as H_2O during the eruption process to maintain a constant CO_2/H_2O ratio in the gas phase. This seems unlikely given the much greater volatility of CO_2 (the vapor pressure of dry ice at its triple point is ~300,500 times larger than that of water ice at this temperature; Lemmon et al., 2010; Haynes, 2014), but this extreme case allows us to determine the maximum effect CO_2 condensation could have on the computed pH. The no distillation case is equivalent to $T_{tiger} = 273$ K in Eq. (2b), which would correspond to $\log(a_{CO2}) = -5.5$ for a CO_2/H_2O ratio of 0.006 in the plume gas (Table 2). This would shift the lower limit on the pH from 10.8 to 9.6 (Fig. 3A). Even in the overly conservative case, the ocean would still be significantly alkaline.

In contrast, the actual pH would be higher than the model-derived value if dry ice or clathrate hydrates (Kieffer et al., 2006) in Enceladus' ice shell are contributing CO_2 to the plume. Less of the observed CO_2 gas would be from the ocean, which would imply a lower activity of CO_2 than adopted. While this hypothesis cannot be ruled out, it does not need to be invoked to account for the presence of CO_2 in the plume because carbonate in the ocean (Postberg et al., 2009) can already provide CO_2 (Eq. (12)). The logarithmic nature of the pH implies that large contributions from dry sources would be required to shift it significantly.

Table 3
Calculated equilibrium speciation of Enceladus' ocean at 0 °C and 1 bar, for a nominal concentration of chloride (0.2 molal) and an intermediate concentration of dissolved inorganic carbon (0.07 molal; see Section 2.3). The columns show molal concentrations for three activities of CO_2 that span a range consistent with the abundance of CO_2 in the plume gas (see Section 2.2). The constrained activity of CO_2 is related to the temperature of the tiger stripes on Enceladus' south polar region via Eq. (2b).

Chemical species	$a_{CO2} = 10^{-11.2}$ ($T_{tiger} = 170$ K)	$a_{CO2} = 10^{-9}$ ($T_{tiger} = 200$ K)	$a_{CO2} = 10^{-7.3}$ ($T_{tiger} = 230$ K)
Na^+	0.345	0.319	0.314
Cl^-	0.2	0.2	0.2
CO_3^{-2}	0.0474	0.0478	0.0451
$NaCO_3^-$	0.0225	0.0215	0.0202
OH^-	0.0279	2.24×10^{-3}	3.08×10^{-4}
HCO_3^-	4×10^{-5}	5.09×10^{-4}	3.51×10^{-3}
NaCl	4.32×10^{-4}	4.06×10^{-4}	4.01×10^{-4}
NaOH	2.68×10^{-3}	2.02×10^{-4}	2.74×10^{-5}
$NaHCO_3$	1.5×10^{-5}	1.79×10^{-4}	1.22×10^{-3}
HCl	3.29×10^{-22}	4.11×10^{-21}	2.99×10^{-20}
pH	13.2	12.1	11.3

On the other hand, the actual pH could be lower than the model-derived value if CO_2 degassing at the top of the ocean is a disequilibrium process. This could occur if droplets of ocean water freeze before they can release sufficient CO_2 (Eq. (12)) to satisfy vapor–liquid equilibrium. In this scenario, the plume should contain more CO_2 gas than it does, which would imply a higher activity of CO_2 than adopted. Such disequilibrium at the ocean-vapor interface seems plausible because the plume particles contain salts (Postberg et al., 2009, 2011), and equilibrium and fractional freezing would exclude salts from the ice (Zolotov, 2007). Flash freezing of ocean water can explain the observations (Spencer and Nimmo, 2013), and if the freezing process is sufficiently rapid, the carbonate system may not achieve equilibrium during the degassing process. However, the system would need to be quite far from equilibrium (i.e., <1% of reaction progress) to appreciably change the computed pH (see above; Eq. (11)), so this may also be a second-order effect.

A final complication could arise if Enceladus' ocean is not well-mixed. In this case, we would be calculating the pH of the uppermost portion of the ocean, where the plume gases are being generated (Schmidt et al., 2008; Hsu et al., 2015). If the rate of degassing is faster than mixing, a compositional gradient would develop. It may be unreasonable to expect complete mixing in the vertical direction because the ocean may be deep (~20–30 km; Iess et al., 2014), compared to the Mariana Trench (~11 km). Degassing of CO_2 raises the pH in the degassing zone (Eq. (12)), so the bulk ocean may have a pH lower than estimated (Fig. 3).

This discussion calls attention to the need for kinetic investigations to understand the consequences of the dynamical balance between freezing, degassing, and mixing (Vance and Goodman, 2009), to clarify how representative the plume's chemistry is to the bulk ocean. In addition, high-precision carbon and oxygen isotope measurements of CO_2 in the plume gas (Waite et al., 2009, 2013) and carbonates in the plume particles (Postberg et al., 2009, 2011) are needed to determine whether these species were previously in equilibrium (Zhang et al., 1995) at the ocean-vapor interface.

Because three of the four secondary effects would lead to a decrease in the pH, it is tempting to assume that the derived value (12.2 ± 1.4; see Section 3.2.2.1) is a slight overestimate. At present, we cannot quantify the possible systematic error because there are four free parameters, but the pH could be about one unit lower than calculated (see Section 4.3).

4. GEOCHEMICAL IMPLICATIONS

4.1. Serpentinization of chondritic rock

The present study represents a top-down approach of inferring the pH from observational data, while the study of Zolotov (2007) represents a bottom-up approach of predicting the pH from physiochemical modeling of expected water–rock interactions that lead to a Na–Cl–CO_3 ocean. The fact that these independent models are converging on a pH of ~11–12 can be taken as an argument that the ocean has this pH. Their consistency also suggests that the assumptions underlying these approaches are appropriate to Enceladus, and provides confidence that they can be used to predict the geochemistry of subsurface oceans (Zolotov and Kargel, 2009) and the composition of possible associated plumes (Roth et al., 2014) on other icy bodies, such as Europa. The general consistency of the pH from the theoretical model with the observationally-derived value can also be taken as evidence that water–rock interactions are the primary controller of the pH of Enceladus' ocean (Zolotov, 2007).

Consistent with the mineralogy of aqueously altered chondrites (Brearley and Jones, 1998; Brearley, 2006), the relatively low density of Enceladus' rocky core (Iess et al., 2014), and experimental (Seyfried et al., 2007) and theoretical (Zolotov, 2007, 2012) simulations, serpentinization (McCollom and Seewald, 2013) can be seen as the key process that led to a high pH ocean on Enceladus. The high pH is a direct consequence of the ultramafic composition of accreted rocks (Jarosewich, 1990). The deduced pH (~11–12) is similar to those (~9–12.5) in hyperalkaline springs from numerous sites of low-temperature (<90 °C) serpentinization on Earth (Barnes et al., 1967, 1978; Kelley et al., 2001, 2005; Mottl et al., 2003; Morrill et al., 2013; Szponar et al., 2013), which bolsters the expectation that serpentinization has occurred on Enceladus (Vance et al., 2007; Malamud and Prialnik, 2013; Tobie, 2015). Thus, serpentinizing systems on Earth, such as the Semail ophiolite in Oman and the Lost City hydrothermal field in the mid-Atlantic Ocean, can be regarded as reasonable geochemical and perhaps biological analogues of the water–rock (ocean-core) system on Enceladus. According to one prominent model (Russell et al., 2010, 2014), the occurrence of serpentinization on Enceladus suggests that this geochemical environment may be conducive to the origin of life. The present study echoes the emerging theme of serpentinization as the most important alteration reaction in the solar system (Brearley, 2006; Schulte et al., 2006; Ehlmann et al., 2010), which suggests that subsurface oceans on other icy worlds in the outer solar system (Hussmann et al., 2006; Castillo-Rogez and McCord, 2010; Robuchon and Nimmo, 2011; Hammond et al., 2013; Baland et al., 2014; Tajeddine et al., 2014) would also be alkaline solutions (Zolotov, 2012).

4.2. Hydrogen generation from iron oxidation

The high pH implies serpentinization (see Section 4.1), and serpentinization is accompanied by the generation of H_2 produced by aqueous oxidation of reduced iron-bearing minerals (Neal and Stanger, 1983; Sleep et al., 2004; Oze and Sharma, 2007; McCollom and Bach, 2009; Klein et al., 2013; Mayhew et al., 2013). This is important because there is the potential to synthesize organic compounds abiotically or biotically from CO_2 or carbonate if there is sufficient H_2 (Shock and McKinnon, 1993; Shock and Canovas, 2010), and H_2-enabled organic synthesis in the interior could explain the presence of organic species in Enceladus' plume (Postberg et al., 2008; Waite et al., 2009, 2013). H_2 would also provide chemical energy that

could support microorganisms, such as methanogens (McCollom, 1999).

The presence of ferric (Fe^{+3}) phases (magnetite, cronstedtite) in aqueously altered chondrites (Brearley, 2006) demonstrates that H_2 was produced on their parent bodies (Rosenberg et al., 2001; Alexander et al., 2010). The occurrence of serpentinization on Enceladus implies that H_2 has been produced inside Enceladus, where the dominant source of H_2 would be the oxidation of accreted metallic iron, which is abundant in primitive bodies (Brearley and Jones, 1998; Zolensky et al., 2006) and unstable in the presence of liquid water at sub-kbar pressures (Glein et al., 2008)

$$3\text{Fe(in kamacite)} + 4H_2O(l) \rightarrow Fe_3O_4\text{(magnetite)} + 4H_2(aq). \quad (15)$$

A simple estimate of the H_2-generating potential of the water–rock system on Enceladus can be made by assuming that the rocky core (7.1×10^{19} kg; Iess et al., 2014) has a total Fe content similar to CI chondrites (~18%), and ~35% of the Fe was accreted as metal, with the remainder as troilite (FeS) and ferrous (Fe^{+2}) silicates (Lodders, 2003). This model could produce 1.1×10^{20} mol of H_2 (Eq. (15)). A total water (liquid + ice) mass of 3.7×10^{19} kg (Iess et al., 2014) leads to a bulk concentration of ~3 mol of H_2 per kg of water (cf. Lost City, ~0.01 molal H_2; Proskurowski et al., 2006). This value illustrates that the water–rock system has the potential to make huge amounts of H_2, as accreted rocks would transfer reducing potential from the H_2-rich solar nebula (Prinn and Fegley, 1989) to Enceladus' interior.

However, the actual concentration of H_2 in the ocean could be much lower than the theoretical maximum if outgassing via the plume (Waite et al., 2011; Brockwell et al., 2014) or other loss processes are depleting the ocean in H_2, or if not all of the reduced Fe minerals have been oxidized (see Section 4.3). As an example, the above endmember scenario implies a mean production rate of H_2 of 775 mol sec^{-1} over the history of the solar system (4.5×10^9 y). A flux of 200 kg (11,100 mol) of water vapor per sec in Enceladus' plume (Hansen et al., 2011) leads to a possible native H_2/H_2O ratio on the order of 10% in the plume gas, which may be detectable to *Cassini* INMS (Brockwell et al., 2014; Bouquet et al., 2015b).

4.3. Extensive alteration and buffering of the ocean

It is unknown whether serpentinization (see Section 4.1) is still occurring on Enceladus. If past hydrothermal processes led to complete serpentinization of the core (Vance et al., 2007), then Enceladus would lack a feedstock of anhydrous and reduced minerals for contemporary serpentinization. This possibility would be consistent with a relatively low core density (2400 kg m^{-3}; Iess et al., 2014) that is similar to those of many phyllosilicate minerals in carbonaceous chondrites (Brearley and Jones, 1998), such as chrysotile serpentine (2500 kg m^{-3}). An anhydrous core may have a density similar to that of Jupiter's moon, Io (3528 kg m^{-3}; Schubert et al., 2007). The hydrostatic core-isostatic ice shell model of Iess et al. (2014) implies that at least most of the core has been serpentinized, but we cannot exclude the possibility of small amounts of unaltered rock (e.g.,<10% of the core mass) in the deepest parts of the core, which may not have a perceptible effect on the gravimetric data (Iess et al., 2014). This hypothesis can be tested by searching for endogenic H_2 in the plume (Brockwell et al., 2014), which would provide evidence for current aqueous alteration processes (Eq. (15); Waite et al., 2013). This is key to assessing the present habitability of Enceladus' ocean (McKay et al., 2014), because there may not be sufficient chemical energy to support life (Schrenk et al., 2013) if H_2 is no longer available (Glein et al., 2008).

The inorganic chemistry of today's ocean is likely to be controlled by equilibria (Sillén, 1961, 1967) between the products of serpentinization, such as phyllosilicates and carbonates, and the aqueous solution. Indeed, equilibrium geochemistry (Zolensky et al., 1989; Zolotov, 2007) can explain why Enceladus' ocean (evidently) has a pH of ~11–12. Recent chemical equilibrium calculations indicate that an ocean floor mineral assemblage of chrysotile–talc–dolomite–calcite–gaylussite in the presence of 0.2 molal Cl^- would buffer the pH = 11.4, $\log(a_{CO2}) = -7.5$, and $m_{DIC} = 0.07$ molal at 0 °C (Glein et al., 2015). These predicted values are consistent with the constraints derived from the observational data (see Sections 2.2 and 2.3). Global-scale equilibrium between sediments and ocean water may occur on Enceladus but not on Earth (Broecker, 1971; Berner and Berner, 1996), because the hydrosphere on Enceladus may be less compositionally heterogeneous (no continental crust) and dynamically disturbed (no solar-driven water cycle or rock cycle driven by plate tectonics) than on Earth. In the absence of large rates of energy input, Enceladus' ocean may equilibrate with many chemical elements in marine sediments over geologic time (apart from kinetically inhibited redox reactions of carbon, nitrogen, sulfur, and possibly iron; Zolotov and Shock, 2004).

4.4. Limited impact of oxidants from the surface

In addition to highlighting the importance of serpentinization, the high ocean pH can rule out or restrict other geochemical processes. For example, it has been hypothesized that strong oxidants (O_2, O_3, H_2O_2) that form on the surfaces of airless icy bodies as a result of photolytic and radiolytic processing of water ice can be delivered to subsurface oceans by resurfacing processes that bury surface materials (Hand et al., 2007). However, Zolotov and Shock (2004) question the significance of oxidant delivery. It is likely that oxidants are produced on the surface of Enceladus (Cooper et al., 2009), because they have been detected on some of Saturn's other icy satellites (Noll et al., 1997; Teolis et al., 2010; Tokar et al., 2012). The more difficult question is whether significant amounts of oxidants have been delivered to Enceladus' ocean. Here, we show that the pH can help address this question because oxidant delivery should lead to a decrease in pH, in response to sulfuric acid production (Pasek and Greenberg, 2012).

The geochemistry of oxidant delivery to oceans on icy moons may parallel acid mine drainage on Earth (Drever, 1997), as exemplified by the following reaction

$$4FeS(troilite) + 10H_2O(l) + 9O_2(aq) \rightarrow 4Fe(OH)_3 \text{ (ferric hydroxide)} + 8H^+(aq) + 4SO_4^{-2}(aq). \quad (16)$$

The combined clues that the ocean is highly alkaline, and sulfate-bearing clusters have not been reported to be present in the plume particles (Postberg et al., 2009, 2011) suggest that the oxidation of metal sulfides to sulfuric acid has not been a quantitatively significant process over the history of Enceladus. This would be thermodynamically consistent with the presence of reduced gases and organic species in Enceladus' plume (Waite et al., 2009, 2011, 2013). Carbonate minerals on the ocean floor (e.g., calcite) could maintain the high pH by neutralizing sulfuric acid, but sulfate would be produced, which has not been detected.

Oxidant delivery may not be important to the geochemistry of Enceladus' ocean because the concentrations of oxidants in surface ices may be low, or the hypothesized delivery mechanism of burying surface materials with plume fallout may be inefficient, particularly if the plume is an episodic phenomenon (Ojakangas and Stevenson, 1986; O'Neill and Nimmo, 2010). These effects would limit the oxidant flux to the ocean, keeping the pH high and sulfate low. A lack of oxidants would constrain sources of chemical energy that could be used by putative life (Gaidos et al., 1999). Alternatively, if oxidant delivery has been robust, then it may look unimportant if life is counteracting Eq. (16) by sulfate reduction (Zolotov and Shock, 2003). This could also explain why the ocean is not more acidic and richer in sulfate, but this process requires the presence of organisms and reductants (e.g., H_2 from serpentinization; see Section 4.2).

5. CONCLUSIONS

We have shown how compositional data on Enceladus' plume from *Cassini* INMS and CDA can be coupled to obtain quantitative information on the geochemistry of Enceladus' ocean. To constrain the composition of the ocean from the plume, our geochemical model accounts for a distillation effect that occurs when water vapor freezes out as gases are transported from the ocean to the surface. Chemical equilibrium calculations show that the ocean should be a Na–Cl–CO_3-type water with a pH of ~11–12 to explain the abundances of CO_2 in the plume gas (Waite et al., 2009; Bouquet et al., 2015a), and sodium chloride and carbonate salts in the plume particles (Postberg et al., 2009, 2011). Enceladus' ocean contains abundant NaCl (~0.2 molal), like terrestrial seawater; but differs from seawater in that Na_2CO_3 (~0.07 molal) replaces $MgSO_4$. Therefore, Enceladus has a soda ocean.

The high pH has the following consequences to the chemical speciation of the ocean: (1) OH^- should be fairly abundant; (2) CO_3^{-2} (or $NaCO_3^-$) should be the dominant form of dissolved inorganic carbon; (3) divalent metals should be present at low concentrations; (4) if present, organic acids should be completely deprotonated; and (5) if present, organic amines should exist mostly in the neutral form. The inferred pH and speciation are considered to be reliable, unless our treatment of the distillation effect is too simplistic because of significant CO_2 condensation, or if the plume formation process exhibits large deviations from phase equilibrium as a result of rapid freezing and/or sluggish mixing of ocean water in the source region. These effects would imply that the estimated pH is an overestimate, but they may be of secondary importance because the log scale makes the pH insensitive to them. The overall conclusion of a high pH ocean should be robust, although the exact value could be debated.

Because the pH is a central compositional variable, it can tell us a great deal about geochemical processes in Enceladus' ocean. We conclude that the high pH is a consequence of serpentinization from interactions between Enceladus' ocean and its chondritic (ultramafic) core. A key implication is that H_2 would be generated during serpentinization, and it can drive the synthesis of organic compounds and provide chemical energy for possible microbial life. However, we do not know whether serpentinization is ongoing or extinct. Enceladus' core may have already been completely serpentinized, and may now be at a state of chemical equilibrium with the ocean. This uncertainty can be resolved by searching for native H_2 in the plume gas, which could be present at a mixing ratio of ~10% with respect to H_2O. Based on the high pH and lack of detection of sulfates, we conclude that significant amounts of water-derived oxidants have not been delivered from the surface to the ocean of Enceladus, possibly because of inefficient delivery as a result of episodic, tidally-driven cryovolcanic activity. As a final point, the highly alkaline pH reported in this study represents evidence of serpentinization on Enceladus, and given the important geochemical and astrobiological implications of serpentinization, we suggest that it would be useful to guide the future exploration of Enceladus around the theme of serpentinization as the driver of its geochemical evolution.

ACKNOWLEDGEMENTS

This paper would not have come to pass without the unprecedented data that have been obtained by the *Cassini* mission, and it was inspired partly by the timeless work of Robert Garrels. C.R.G. is grateful to George Cody, Matthieu Galvez, Conel Alexander, Frank Postberg, Jonathan Lunine, and Barbara Sherwood Lollar for many interesting discussions and their encouragement. He would also like to express his gratitude to the Deep Carbon Observatory, and to the Carnegie Institution and NASA Astrobiology Institute for supporting his postdoctoral fellowship. C.R.G. and J.A.B. thank the Enceladus LIFE team (especially Peter Tsou and Ariel Anbar) for many pedagogical discussions about a sample return mission to Enceladus. J.A.B. acknowledges funding from NASA Astrobiology Institute Grant through Cooperative Agreement NNA04CC09A to the Geophysical Laboratory of the Carnegie Institution for Science. J.H.W. acknowledges funding from the Cassini Project (contract number NAS703001TONMO711123). We thank Misha Zolotov and an anonymous reviewer for helpful comments, and Eric Quirico for careful editorial handling. This paper began as a presentation at the first Enceladus LIFE Workshop, and benefited from the stimulating atmosphere at the meeting. Subsequent discussions at the

Europa Clipper Plume Advisory Session helped to refine our ideas. C.R.G. dedicates his contribution to this paper to S.I.G.

APPENDIX

Explanation of the updated CO_2 abundance

Since the publication of Waite et al. (2009) that reported results from the E5 flyby in 2008, the plume gas has been measured by *Cassini* INMS during flybys E7, E14, E17, and E18 from 2009 to 2012. The composition of the gas is obtained from the mass spectrum using the forward modeling methodology of Magee et al. (2009), which deconvolves mass peaks from parent species and their fragmentation products. The result is a set of species and their mixing ratios that provide a best-fit (reduced chi-squared) to the observed mass spectrum.

Preliminary results on the plume gas composition from the more recent flybys have been reported by Waite et al. (2011, 2013), and the full dataset will be reported by Magee, Waite, and colleagues in a future publication. Here, we discuss how the new results lead to a revision in the CO_2/H_2O molar ratio, which is a key observational constraint to modeling the carbonate geochemistry of Enceladus' ocean.

The general result is that the observed composition is strongly dependent on the flyby velocity. E5 had a flyby velocity of $\sim$18 km sec^{-1}, while the more recent flybys had velocities of $\sim$8 km sec^{-1}. The data from the slower flybys are considered to more closely reflect the composition of the plume gas because they give repeatable results, and molecular fragmentation by impacts on the INMS antechamber becomes more important at higher velocities (Waite et al., 2009). An important consequence of the impact chemistry is that the mixing ratio of CO is found to increase with flyby velocity. Waite et al. (2009) initially attributed this effect to the dissociation of CO_2 to CO in the INMS antechamber. Based on this assumption, they estimated the CO_2 mixing ratio ($5.3 \pm 0.1\%$) in the unmodified plume gas by summing the modeled mixing ratios of CO_2 (0.9%) and CO (4.4%). The new data, however, show that this assumption is incorrect, and there must be a different source of CO at high velocity (Waite et al., 2011, 2013). The best-fit mixing ratios for CO_2 and H_2O in the plume gas are $0.52 \pm 0.01\%$ and $87 \pm 0.7\%$, respectively, at low velocity (Bouquet et al., 2015a). These values lead to the CO_2/H_2O ratio of 0.006 that is used in the present paper (Table 2).

REFERENCES

Alexander C. M. O'D. et al. (2010) Deuterium enrichments in chondritic macromolecular material – Implications for the origin and evolution of organics, water and asteroids. *Geochim. Cosmochim. Acta* **74**, 4417–4437.

Alexander C. M. O'D. et al. (2015) Carbonate abundances and isotopic compositions in chondrites. *Meteorit. Planet. Sci.* **50**, 810–833.

Anderson G. M. (2005) *Thermodynamics of Natural Systems*. Cambridge Univ. Press, New York.

Baland R.-M. et al. (2014) Titan's internal structure inferred from its gravity field, shape, and rotation state. *Icarus* **237**, 29–41.

Barnes I. et al. (1967) Geochemical evidence of present-day serpentinization. *Science* **156**, 830–832.

Barnes I. et al. (1978) Present day serpentinization in New Caledonia, Oman and Yugoslavia. *Geochim. Cosmochim. Acta* **42**, 144–145.

Běhounková M. et al. (2012) Tidally-induced melting events as the origin of south-pole activity on Enceladus. *Icarus* **219**, 655–664.

Berner E. K. and Berner R. A. (1996) *Global Environment: Water, Air, and Geochemical Cycles*. Prentice Hall, Upper Saddle River, NJ.

Bethke C. M. (2008) *Geochemical and Biogeochemical Reaction Modeling*. Cambridge Univ. Press, New York.

Bischoff J. L. et al. (1991) Gaylussite formation at Mono Lake, California. *Geochim. Cosmochim. Acta* **55**, 1743–1747.

Bischoff J. L. et al. (1993) Ikaite precipitation by mixing of shoreline springs and lake water, Mono Lake, California, USA. *Geochim. Cosmochim. Acta* **57**, 3855–3865.

Bockelée-Morvan D. et al. (2014) Searches for HCl and HF in comets 103P/Hartley 2 and C/2009 P1 (Garradd) with the Herschel Space Observatory. *Astron. Astrophys.* **562**, A5. http://dx.doi.org/10.1051/0004-6361/201322939.

Bouquet A. et al. (2015a) Possible evidence for a methane source in Enceladus' ocean. *Geophys. Res. Lett.* **42**. http://dx.doi.org/10.1002/2014GL063013.

Bouquet A., et al. (2015b) Evaluating the quantity of native H_2 in Enceladus' plumes. *Lunar Planet. Sci. XLVI*. #2320 (abstr.).

Bowers T. S. et al. (1984) *Equilibrium Activity Diagrams for Coexisting Minerals and Aqueous Solutions at Pressures and Temperatures to 5 kb and 600°C*. Springer-Verlag, New York.

Brearley A. J. (2006) The action of water. In *Meteorites and the Early Solar System II* (eds. D. S. Lauretta and H. Y. McSween). Univ. of Arizona Press, Tucson, AZ, pp. 587–624.

Brearley A. J. and Jones R. H. (1998) Chondritic meteorites. In *Planetary Materials* (ed. J. J. Papike). Mineral. Soc. of Am., Washington, DC, pp. 3-1–3-98.

Brockwell T. G., et al. (2014) Hydrogen in Enceladus' plume – Native or artifact? *Workshop on the Habitability of Icy Worlds*. #4022 (abstr.).

Broecker W. S. (1971) A kinetic model for the chemical composition of sea water. *Quatern. Res.* **1**, 188–207.

Brown R. H. et al. (2006) Composition and physical properties of Enceladus' surface. *Science* **311**, 1425–1428.

Castillo-Rogez J. C. and McCord T. B. (2010) Ceres' evolution and present state constrained by shape data. *Icarus* **205**, 443–459.

Choi J. et al. (1998) Modeling CO_2 degassing and pH in a stream-aquifer system. *J. Hydrol.* **209**, 297–310.

Christner B. C. et al. (2014) A microbial ecosystem beneath the West Antarctic ice sheet. *Nature* **512**, 310–313.

Cody G. D. et al. (2011) Establishing a molecular relationship between chondritic and cometary organic solids. *Proc. Natl. Acad. Sci. USA* **108**, 19171–19176.

Collins G. C. and Goodman J. C. (2007) Enceladus' south polar sea. *Icarus* **189**, 72–82.

Cooper J. F. et al. (2009) Old Faithful model for radiolytic gas-driven cryovolcanism at Enceladus. *Planet. Space Sci.* **57**, 1607–1620.

Dachwald B. et al. (2014) IceMole: A maneuverable probe for clean in situ analysis and sampling of subsurface ice and subglacial aquatic ecosystems. *Ann. Glaciol.* **55**, 14–22.

Deocampo D. M. and Jones B. F. (2014) Geochemistry of saline lakes. In *Surface and Groundwater, Weathering and Soils* (ed. J. I. Drever), *Treatise on Geochemistry*, second ed., vol. 7. Elsevier, Amsterdam. pp. 437–469.

Drever J. I. (1997) *The Geochemistry of Natural Waters: Surface and Groundwater Environments*. Prentice Hall, Upper Saddle River, NJ.

Ehlmann B. L. et al. (2010) Geologic setting of serpentine deposits on Mars. *Geophys. Res. Lett.* **37**, L06201. http://dx.doi.org/10.1029/2010GL042596.

Elsila J. E. et al. (2009) Cometary glycine detected in samples returned by Stardust. *Meteorit. Planet. Sci.* **44**, 1323–1330.

Eugster H. P. and Hardie L. A. (1978) Saline lakes. In *Lakes: Chemistry, Geology, Physics* (ed. A. Lerman). Springer-Verlag, New York, pp. 237–293.

Gaidos E. J. et al. (1999) Life in ice-covered oceans. *Science* **284**, 1631–1633.

Garrels R. M. and Christ C. L. (1965) Solutions, Minerals, and Equilibria. Freeman, Cooper & Company, San Francisco, CA.

Garrels R. M. and Mackenzie F. T. (1967) Origin of the chemical compositions of some springs and lakes. In *Equilibrium Concepts in Natural Water Systems* (ed. W. Stumm). Am. Chem. Soc, Washington, DC, pp. 222–242.

Garrels R. M. and Thompson M. E. (1962) A chemical model for sea water at 25°C and one atmosphere total pressure. *Am. J. Sci.* **260**, 57–66.

Glavin D. P. et al. (2008) Detection of cometary amines in samples returned by Stardust. *Meteorit. Planet. Sci.* **43**, 399–413.

Glein C. R. (2015) Noble gases, nitrogen, and methane from the deep interior to the atmosphere of Titan. *Icarus* **250**, 570–586.

Glein C. R. and Shock E. L. (2010) Sodium chloride as a geophysical probe of a subsurface ocean on Enceladus. *Geophys. Res. Lett.* **37**, L09204. http://dx.doi.org/10.1029/2010GL042446.

Glein C. R. et al. (2008) The oxidation state of hydrothermal systems on early Enceladus. *Icarus* **197**, 157–163.

Glein C. R. et al. (2009) The absence of endogenic methane on Titan and its implications for the origin of atmospheric nitrogen. *Icarus* **204**, 637–644.

Glein C. R., et al. (2015) The chemistry of Enceladus' ocean from a convergence of Cassini data and theoretical geochemistry. *Lunar Planet. Sci. XLVI*. #1685 (abstr.).

Goguen J. D. et al. (2013) The temperature and width of an active fissure on Enceladus measured with Cassini VIMS during the 14 April 2012 South Pole flyover. *Icarus* **226**, 1128–1137.

Grady M. M. et al. (2002) Light element geochemistry of the Tagish Lake CI2 chondrite: Comparison with CI1 and CM2 meteorites. *Meteorit. Planet. Sci.* **37**, 713–735.

Grotzinger J. P. et al. (2014) A habitable fluvio-lacustrine environment at Yellowknife Bay, Gale Crater, Mars. *Science* **343**, 1242777. http://dx.doi.org/10.1126/science.1242777.

Hammer O. et al. (2005) Evolution of fluid chemistry during travertine formation in the Troll thermal springs, Svalbard, Norway. *Geofluids* **5**, 140–150.

Hammond N. P. et al. (2013) Flexure on Dione: Investigating subsurface structure and thermal history. *Icarus* **223**, 418–422.

Hand K. P. et al. (2007) Energy, chemical disequilibrium, and geological constraints on Europa. *Astrobiology* **7**, 1006–1022.

Hansen C. J. and Kirk R. (2015) Triton's plumes – Solar-driven like Mars or endogenic like Enceladus? *Lunar Planet. Sci. XLVI*. #2423 (abstr.).

Hansen C. J. et al. (2006) Enceladus' water vapor plume. *Science* **311**, 1422–1425.

Hansen C. J. et al. (2011) The composition and structure of the Enceladus plume. *Geophys. Res. Lett.* **38**, L11202. http://dx.doi.org/10.1029/2011GL047415.

Haynes, W. M. (ed.) (2014) *CRC Handbook of Chemistry and Physics (Internet Version 2014)*, 94th ed. CRC Press/Taylor and Francis, Boca Raton, FL.

Hedman M. M. et al. (2013) An observed correlation between plume activity and tidal stresses on Enceladus. *Nature* **500**, 182–184.

Helgeson H. C. (1969) Thermodynamics of hydrothermal systems at elevated temperatures and pressures. *Am. J. Sci.* **267**, 729–804.

Holland H. D. (1984) *The Chemical Evolution of the Atmosphere and Oceans*. Princeton Univ. Press, Princeton, NJ.

Howett C. J. A. et al. (2011) High heat flow from Enceladus' south polar region measured using 10–600 cm^{-1} Cassini/CIRS data. *J. Geophys. Res.* **116**, E03003. http://dx.doi.org/10.1029/2010JE003718.

Hsu H.-W. et al. (2015) Ongoing hydrothermal activities within Enceladus. *Nature* **519**, 207–210.

Hussmann H. et al. (2006) Subsurface oceans and deep interiors of medium-sized outer planet satellites and large trans-neptunian objects. *Icarus* **185**, 258–273.

Iess L. et al. (2014) The gravity field and interior structure of Enceladus. *Science* **344**, 78–80.

Ingersoll A. P. and Pankine A. A. (2010) Subsurface heat transfer on Enceladus: Conditions under which melting occurs. *Icarus* **206**, 594–607.

Ingersoll A. P. and Ewald S. P. (2011) Total particulate mass in Enceladus plumes and mass of Saturn's E ring inferred from Cassini ISS images. *Icarus* **216**, 492–506.

Jarosewich E. (1990) Chemical analyses of meteorites: A compilation of stony and iron meteorite analyses. *Meteoritics* **25**, 323–337.

Johnson J. W. et al. (1992) SUPCRT92: A software package for calculating the standard molal thermodynamic properties of minerals, gases, aqueous species, and reactions from 1 to 5000 bar and 0 to 1000°C. *Comput. Geosci.* **18**, 899–947.

Jones B. F. et al. (1977) Hydrochemistry of the Lake Magadi basin, Kenya. *Geochim. Cosmochim. Acta* **41**, 53–72.

Jones G. H. et al. (2009) Fine jet structure of electrically charged grains in Enceladus' plume. *Geophys. Res. Lett.* **36**, L16204. http://dx.doi.org/10.1029/2009GL038284.

Kargel J. S. et al. (2000) Europa's crust and ocean: Origin, composition, and the prospects for life. *Icarus* **148**, 226–265.

Kelley D. S. et al. (2001) An off-axis hydrothermal vent field near the Mid-Atlantic Ridge at 30°N. *Nature* **412**, 145–149.

Kelley D. S. et al. (2005) A serpentinite-hosted ecosystem: The Lost City hydrothermal field. *Science* **307**, 1428–1434.

Kempe S. and Kazmierczak J. (2002) Biogenesis and early life on Earth and Europa: Favored by an alkaline ocean? *Astrobiology* **2**, 123–130.

Kieffer S. W. et al. (2006) A clathrate reservoir hypothesis for Enceladus' south polar plume. *Science* **314**, 1764–1766.

Kirby J. P., et al. (2014) Enceladus remote organic detection: Aerogel ice particle collection and in situ mass spectrometer analysis. *Workshop on the Habitability of Icy Worlds*. #4076 (abstr.).

Klein F. et al. (2013) Compositional controls on hydrogen generation during serpentinization of ultramafic rocks. *Lithos* **178**, 55–69.

Küppers M. et al. (2014) Localized sources of water vapour on the dwarf planet (1)Ceres. *Nature* **505**, 525–527.

Lang S. Q. et al. (2010) Elevated concentrations of formate, acetate and dissolved organic carbon found at the Lost City hydrothermal field. *Geochim. Cosmochim. Acta* **74**, 941–952.

Lemmon E. W., et al. (2010) *NIST Standard Reference Database 23: Reference Fluid Thermodynamic and Transport Properties-REFPROP*, Version 9.0. National Institute of Standards and Technology, Standard Reference Data Program, Gaithersburg, MD.

Lodders K. (2003) Solar system abundances and condensation temperatures of the elements. *Astrophys. J.* **591**, 1220–1247.

Lunine J. I., et al. (2015) Enceladus Life Finder: The search for life in a habitable moon. *Lunar Planet. Sci. XLVI.* #1525 (abstr.).

Macke R. J. et al. (2011) Density, porosity, and magnetic susceptibility of carbonaceous chondrites. *Meteorit. Planet. Sci.* **46**, 1842–1862.

Magee B. A. et al. (2009) INMS-derived composition of Titan's upper atmosphere: Analysis methods and model comparison. *Planet. Space Sci.* **57**, 1895–1916.

Malamud U. and Prialnik D. (2013) Modeling serpentinization: Applied to the early evolution of Enceladus and Mimas. *Icarus* **225**, 763–774.

Marion G. M. et al. (2005) Effects of pressure on aqueous chemical equilibria at subzero temperatures with applications to Europa. *Geochim. Cosmochim. Acta* **69**, 259–274.

Marion G. M. et al. (2010) FREZCHEM: A geochemical model for cold aqueous solutions. *Comput. Geosci.* **36**, 10–15.

Marion G. M. et al. (2012) Modeling ammonia-ammonium aqueous chemistries in the Solar System's icy bodies. *Icarus* **220**, 932–946.

Matson D. L. et al. (2007) Enceladus' plume: Compositional evidence for a hot interior. *Icarus* **187**, 569–573.

Matson D. L. et al. (2012) Enceladus: A hypothesis for bringing both heat and chemicals to the surface. *Icarus* **221**, 53–62.

Mayhew L. E. et al. (2013) Hydrogen generation from low-temperature water–rock reactions. *Nat. Geosci.* **6**, 478–484.

McCollom T. M. (1999) Methanogenesis as a potential source of chemical energy for primary biomass production by autotrophic organisms in hydrothermal systems on Europa. *J. Geophys. Res.-Planet.* **104**, 30729–30742.

McCollom T. M. and Bach W. (2009) Thermodynamic constraints on hydrogen generation during serpentinization of ultramafic rocks. *Geochim. Cosmochim. Acta* **73**, 856–875.

McCollom T. M. and Seewald J. S. (2013) Serpentinites, hydrogen, and life. *Elements* **9**, 129–134.

McKay C. P. et al. (2008) The possible origin and persistence of life on Enceladus and detection of biomarkers in the plume. *Astrobiology* **8**, 909–919.

McKay C. P. et al. (2014) Follow the plume: The habitability of Enceladus. *Astrobiology* **14**, 352–355.

Morrill P. L. et al. (2013) Geochemistry and geobiology of a present-day serpentinization site in California: The Cedars. *Geochim. Cosmochim. Acta* **109**, 222–240.

Mottl M. J. et al. (2003) Deep-slab fluids fuel extremophilic Archaea on a Mariana forearc serpentinite mud volcano: Ocean Drilling Program Leg 195. *Geochem. Geophys. Geosys.* **4**, 9009. http://dx.doi.org/10.1029/2003GC000588.

Murray A. E. et al. (2012) Microbial life at −13°C in the brine of an ice-sealed Antarctic lake. *Proc. Natl. Acad. Sci. USA* **109**, 20626–20631.

Neal C. and Stanger G. (1983) Hydrogen generation from mantle source rocks in Oman. *Earth Planet. Sci. Lett.* **66**, 315–320.

Neubeck A. et al. (2014) Olivine alteration and H_2 production in carbonate-rich, low temperature aqueous environments. *Planet. Space Sci.* **96**, 51–61.

Neveu M. et al. (2015) Prerequisites for explosive cryovolcanism on dwarf planet-class Kuiper belt objects. *Icarus* **246**, 48–64.

Nimmo F. et al. (2007) Shear heating as the origin of the plumes and heat flux on Enceladus. *Nature* **447**, 289–291.

Nimmo F. et al. (2014) Tidally modulated eruptions on Enceladus: Cassini ISS observations and models. *Astron. J.* **148**, 46. http://dx.doi.org/10.1088/0004-6256/148/3/46.

Noll K. S. et al. (1997) Detection of ozone on Saturn's satellites Rhea and Dione. *Nature* **388**, 45–47.

Ojakangas G. W. and Stevenson D. J. (1986) Episodic volcanism of tidally heated satellites with application to Io. *Icarus* **66**, 341–358.

O'Neill C. and Nimmo F. (2010) The role of episodic overturn in generating the surface geology and heat flow on Enceladus. *Nat. Geosci.* **3**, 88–91.

Ootsubo T. et al. (2012) AKARI near-infrared spectroscopic survey for CO_2 in 18 comets. *Astrophys. J.* **752**, 15. http://dx.doi.org/10.1088/0004-637X/752/1/15.

Oze C. and Sharma M. (2007) Serpentinization and the inorganic synthesis of H_2 in planetary surfaces. *Icarus* **186**, 557–561.

Pappalardo R. T. et al. (2013) Science potential from a Europa lander. *Astrobiology* **13**, 740–773.

Pappalardo R. T., et al. (2015) Science and reconnaissance from the Europa Clipper mission concept: Exploring Europa's habitability. *Lunar Planet. Sci. XLVI.* #2673 (abstr.).

Parkinson C. D. et al. (2008) Habitability of Enceladus: Planetary conditions for life. *Orig. Life Evol. Biosph.* **38**, 355–369.

Pasek M. A. and Greenberg R. (2012) Acidification of Europa's subsurface ocean as a consequence of oxidant delivery. *Astrobiology* **12**, 151–159.

Pizzarello S. et al. (2006) The nature and distribution of the organic material in carbonaceous chondrites and interplanetary dust particles. In *Meteorites and the Early Solar System II* (eds. D. S. Lauretta and H. Y. McSween). Univ. of Arizona Press, Tucson, AZ, pp. 625–651.

Pope E. C. et al. (2012) Isotope composition and volume of Earth's early oceans. *Proc. Natl. Acad. Sci. USA* **109**, 4371–4376.

Porco C. C. et al. (2006) Cassini observes the active south pole of Enceladus. *Science* **311**, 1393–1401.

Porco C. et al. (2014) How the geysers, tidal stresses, and thermal emission across the south polar terrain of Enceladus are related. *Astron. J.* **148**, 45. http://dx.doi.org/10.1088/0004-6256/148/3/45.

Postberg F. et al. (2008) The E-ring in the vicinity of Enceladus: II. Probing the moon's interior – The composition of E-ring particles. *Icarus* **193**, 438–454.

Postberg F. et al. (2009) Sodium salts in E-ring ice grains from an ocean below the surface of Enceladus. *Nature* **459**, 1098–1101.

Postberg F. et al. (2011) A salt-water reservoir as the source of a compositionally stratified plume on Enceladus. *Nature* **474**, 620–622.

Prinn R. G. and Fegley B. (1989) Solar nebula chemistry: Origin of planetary, satellite, and cometary volatiles. In *Origin and Evolution of Planetary and Satellite Atmospheres* (eds. S. K. Atreya, J. B. Pollack and M. S. Matthews). Univ. of Arizona Press, Tucson, AZ, pp. 78–136.

Proskurowski G. et al. (2006) Low temperature volatile production at the Lost City Hydrothermal Field, evidence from a hydrogen stable isotope geothermometer. *Chem. Geol.* **229**, 331–343.

Proskurowski G. et al. (2008) Abiogenic hydrocarbon production at Lost City hydrothermal field. *Science* **319**, 604–607.

Roberts J. H. and Nimmo F. (2008) Tidal heating and the long-term stability of a subsurface ocean on Enceladus. *Icarus* **194**, 675–689.

Robuchon G. and Nimmo F. (2011) Thermal evolution of Pluto and implications for surface tectonics and a subsurface ocean. *Icarus* **216**, 426–439.

Rosenberg N. D. et al. (2001) Modeling aqueous alteration of CM carbonaceous chondrites. *Meteorit. Planet. Sci.* **36**, 239–244.

Roth L. et al. (2014) Transient water vapor at Europa's south pole. *Science* **343**, 171–174.

Russell M. J. et al. (2010) Serpentinization as a source of energy at the origin of life. *Geobiology* **8**, 355–371.

Russell M. J. et al. (2014) The drive to life on wet and icy worlds. *Astrobiology* **14**, 308–343.

Schmidt J. et al. (2008) Slow dust in Enceladus' plume from condensation and wall collisions in tiger stripe fractures. *Nature* **451**, 685–688.

Schrenk M. O. et al. (2013) Serpentinization, carbon, and deep life. In *Carbon in Earth* (eds. R. M. Hazen, A. P. Jones and J. A. Baross). Mineral. Soc. of Am, Chantilly, VA, pp. 575–606.

Schubert G. et al. (2007) Enceladus: Present internal structure and differentiation by early and long-term radiogenic heating. *Icarus* **188**, 345–355.

Schulte M. and Shock E. (2004) Coupled organic synthesis and mineral alteration on meteorite parent bodies. *Meteorit. Planet. Sci.* **39**, 1577–1590.

Schulte M. et al. (2006) Serpentinization and its implications for life on the early Earth and Mars. *Astrobiology* **6**, 364–376.

Seyfried W. E. et al. (2007) Redox evolution and mass transfer during serpentinization: An experimental and theoretical study at 200°C, 500 bar with implications for ultramafic-hosted hydrothermal systems at mid-ocean ridges. *Geochim. Cosmochim. Acta* **71**, 3872–3886.

Sharp Z. D. and Draper D. S. (2013) The chlorine abundance of Earth: Implications for a habitable planet. *Earth Planet. Sci. Lett.* **369**, 71–77.

Shock E. L. (1995) Organic acids in hydrothermal solutions: Standard molal thermodynamic properties of carboxylic acids and estimates of dissociation constants at high temperatures and pressures. *Am. J. Sci.* **295**, 496–580.

Shock E. and Canovas P. (2010) The potential for abiotic organic synthesis and biosynthesis at seafloor hydrothermal systems. *Geofluids* **10**, 161–192.

Shock E. L. and Koretsky C. M. (1993) Metal-organic complexes in geochemical processes: Calculation of standard partial molal thermodynamic properties of aqueous acetate complexes at high pressures and temperatures. *Geochim. Cosmochim. Acta* **57**, 4899–4922.

Shock E. L. and McKinnon W. B. (1993) Hydrothermal processing of cometary volatiles – Applications to Triton. *Icarus* **106**, 464–477.

Shock E. L. et al. (1989) Calculation of the thermodynamic and transport properties of aqueous species at high pressures and temperatures: Standard partial molal properties of inorganic neutral species. *Geochim. Cosmochim. Acta* **53**, 2157–2183.

Shock E. L. et al. (1997) Inorganic species in geologic fluids: Correlations among standard molal thermodynamic properties of aqueous ions and hydroxide complexes. *Geochim. Cosmochim. Acta* **61**, 907–950.

Sillén L. G. (1961) The physical chemistry of sea water. In *Oceanography* (ed. M. Sears). Am. Assoc. for the Adv. of Sci, Washington, DC, pp. 549–581.

Sillén L. G. (1967) The ocean as a chemical system. *Science* **156**, 1189–1197.

Sleep N. H. et al. (2004) H_2-rich fluids from serpentinization: Geochemical and biotic implications. *Proc. Natl. Acad. Sci. USA* **101**, 12818–12823.

Smith B. A. et al. (1982) A new look at the Saturn system: The Voyager 2 images. *Science* **215**, 504–537.

Sohl F. et al. (2010) Subsurface water oceans on icy satellites: Chemical composition and exchange processes. *Space Sci. Rev.* **153**, 485–510.

Sorokin D. Y. et al. (2014) Microbial diversity and biogeochemical cycling in soda lakes. *Extremophiles* **18**, 791–809.

Sotin C., et al. (2011) JET: Journey to Enceladus and Titan. *Lunar Planet. Sci. XLII*. #1326 (abstr.).

Spencer J. R. and Nimmo F. (2013) Enceladus: An active ice world in the Saturn system. *Annu. Rev. Earth Planet. Sci.* **41**, 693–717.

Spencer J. R. et al. (2006) Cassini encounters Enceladus: Background and the discovery of a south polar hot spot. *Science* **311**, 1401–1405.

Spencer J. R. et al. (2009) Enceladus: An active cryovolcanic satellite. In *Saturn from Cassini-Huygens* (eds. M. K. Dougherty, L. W. Esposito and S. M. Krimigis). Springer, New York, pp. 683–724.

Spitale J. N. and Porco C. C. (2007) Association of the jets of Enceladus with the warmest regions on its south-polar fractures. *Nature* **449**, 695–697.

Stumm W. and Morgan J. J. (1996) *Aquatic Chemistry: Chemical Equilibria and Rates in Natural Waters*. John Wiley & Sons, New York.

Sverjensky D. A. and Lee N. (2010) The great oxidation event and mineral diversification. *Elements* **6**, 31–36.

Szponar N. et al. (2013) Geochemistry of a continental site of serpentinization, the Tablelands Ophiolite, Gros Morne National Park: A Mars analogue. *Icarus* **224**, 286–296.

Tajeddine R. et al. (2014) Constraints on Mimas' interior from Cassini ISS libration measurements. *Science* **346**, 322–324.

Teolis B. D. et al. (2010) Cassini finds an oxygen-carbon dioxide atmosphere at Saturn's icy moon Rhea. *Science* **330**, 1813–1815.

Tobie G. (2015) Planetary science. Enceladus' hot springs. *Nature* **519**, 162–163.

Tobie G. et al. (2008) Solid tidal friction above a liquid water reservoir as the origin of the south pole hotspot on Enceladus. *Icarus* **196**, 642–652.

Tokar R. L. et al. (2012) Detection of exospheric O_2^+ at Saturn's moon Dione. *Geophys. Res. Lett.* **39**, L03105. http://dx.doi.org/10.1029/2011GL050452.

Travis B. J. and Schubert G. (2015) Keeping Enceladus warm. *Icarus* **250**, 32–42.

Tsou P. et al. (2012) LIFE: Life Investigation for Enceladus: A sample return mission concept in search for evidence of life. *Astrobiology* **12**, 730–742.

Vance S. and Goodman J. (2009) Oceanography of an ice-covered moon. In *Europa* (eds. R. T. Pappalardo, W. B. McKinnon and K. K. Khurana). Univ. of Arizona Press, Tucson, AZ, pp. 459–482.

Vance S. et al. (2007) Hydrothermal systems in small ocean planets. *Astrobiology* **7**, 987–1005.

Waite J. H. et al. (2006) Cassini Ion and Neutral Mass Spectrometer: Enceladus plume composition and structure. *Science* **311**, 1419–1422.

Waite J. H. et al. (2009) Liquid water on Enceladus from observations of ammonia and ^{40}Ar in the plume. *Nature* **460**, 487–490.

Waite J. H., et al. (2011) Enceladus plume composition. *EPSC-DPS Joint Meeting*. #61 (abstr.).

Waite J. H., et al. (2013) Enceladus plume composition. *Am. Geophys. Union Fall Meeting*. #P53E-08 (abstr.).

Yeoh S. K. et al. (2015) On understanding the physics of the Enceladus south polar plume via numerical simulation. *Icarus* **253**, 205–222.

Yuen G. et al. (1984) Carbon isotope composition of low molecular weight hydrocarbons and monocarboxylic acids from Murchison meteorite. *Nature* **307**, 252–254.

Zhang J. et al. (1995) Carbon isotope fractionation during gas-water exchange and dissolution of CO_2. *Geochim. Cosmochim. Acta* **59**, 107–114.

Zolensky M. E. et al. (1989) Aqueous alteration on the hydrous asteroids: Results of EQ3/6 computer simulations. *Icarus* **78**, 411–425.

Zolensky M. E. et al. (1999) Asteroidal water within fluid inclusion-bearing halite in an H5 chondrite, Monahans (1998). *Science* **285**, 1377–1379.

Zolensky M. E. et al. (2006) Mineralogy and petrology of Comet 81P/Wild 2 nucleus samples. *Science* **314**, 1735–1739.

Zolotov M. Y. (2007) An oceanic composition on early and today's Enceladus. *Geophys. Res. Lett.* **34**, L23203. http://dx.doi.org/10.1029/2007GL031234.

Zolotov M. Y. (2012) Aqueous fluid composition in CI chondritic materials: Chemical equilibrium assessments in closed systems. *Icarus* **220**, 713–729.

Zolotov M. Y. (2014) Formation of brucite and cronstedtite-bearing mineral assemblages on Ceres. *Icarus* **228**, 13–26.

Zolotov M. Y. and Kargel J. S. (2009) On the chemical composition of Europa's icy shell, ocean, and underlying rocks. In *Europa* (eds. R. T. Pappalardo, W. B. McKinnon and K. K. Khurana). Univ. of Arizona Press, Tucson, AZ, pp. 431–457.

Zolotov M. Y. and Postberg F. (2014) Can nano-phase silica originate from chondritic fluids? The application to Enceladus' SiO_2 particles. *Lunar Planet. Sci. XLV*. #2496 (abstr.).

Zolotov M. Y. and Shock E. L. (2003) Energy for biologic sulfate reduction in a hydrothermally formed ocean on Europa. *J. Geophys. Res.* **108**, 5022. http://dx.doi.org/10.1029/2002JE001966.

Zolotov M. Y. and Shock E. L. (2004) A model for low-temperature biogeochemistry of sulfur, carbon, and iron on Europa. *J. Geophys. Res.* **109**, E06003. http://dx.doi.org/10.1029/2003JE002194.

Associate editor: Eric Quirico